The lectin-like TNF Domain:
Role in Experimental Models of Pulmonary Edema Reabsorption and *Trypanosoma brucei* Infection

DISSERTATION

zur Erlangung des akademischen Grades eines
Doktors der Naturwissenschaften (Dr. rer. nat.)
des Fachbereichs für Biologie
an der Universität Konstanz

vorgelegt von
Astrid Leja

Tag der mündlichen Prüfung: 23.11.04
1. Referent: Prof. Dr. Albrecht Wendel
2. Referent: Prof. Dr. Horst Bluethmann

Danksagung

Die vorliegende Arbeit wurde unter der Leitung von Herrn Professor Albrecht Wendel am Lehrstuhl für biochemische Pharmakologie im Fachbereich Biologie der Universität Konstanz angefertigt. Ihm gilt mein besonderer Dank für die Unterstützung dieser Arbeit, für die Schaffung hervorragender Arbeitsbedingungen innerhalb der Arbeitsgruppe, sowie für die Möglichkeit eigenverantwortlich zu arbeiten.

Herzlich bedanken möchte ich mich bei Herrn Dr. Rudolf Lucas für die Bereitstellung des Themas, seine Diskussionsbereitschaft und die immer freundliche und freundschaftliche Begleitung.

Für die hervorragende wissenschaftliche Betreuung dieser Arbeit gilt mein besonderer Dank Dr. Thomas Meergans. Durch seine konstruktive Kritik und seine ständige Bereitschaft zu Diskussionen und Problemfindungen entstanden immer wieder Anregungen für experimentelle Verbesserungen und weiterführende Versuche.

Als Mitglied des Graduiertenkollegs für biomedizinische Wirkstoff-Forschung hatte ich die Möglichkeit an exzellenten Fortbildungskursen und Seminaren teilzunehmen. Dadurch lernte ich viel Neues kennen und erhielt wertvolle Anregungen auch über mein eigenes Forschungsgebiet hinaus. Die Kontakte und Freundschaften im Graduiertenkolleg haben die Zeit der Promotion sehr bereichert und werden sicherlich auch darüber hinaus Bestand haben.

Ein großer Dank an die gesamte Arbeitsgruppe für die gute Zusammenarbeit und die angenehme Atmosphäre. Besonders danke ich Verena, Anne, Sabine, Michael und Markus für die freundschaftliche Atmosphäre auch über die Arbeit hinaus.

Ein riesengroßes Dankeschön an meine Eltern für die fortwährende persönliche Unterstützung.

Markus danke ich dafür, dass er wie selbstverständlich immer für mich da ist.

Table of Contents

ENaC	epithelial sodium channel
ESC	embryonic stem cell
HAT	human sleeping sickness
LPS	lipopolysaccharide
PEEP	positive end-expiratory pressure
k.i.	knock in
MF	murine fibroblast
SEM	standard error of means
TACE	TNFα converting enzyme
TGF	transforming growth factor
TNF	tumor necrosis factor
TNFR	TNF receptor
TRAF	TNF-R-associated factor 2
TV	tidal volume
wt	wild type

1. Introduction

1.1 TNF

The cytokine tumor necrosis factor is a molecule with a dual history. On the one hand, it was isolated as "cachectin", a mediator implicated in the pathogenesis of wasting and responsible for the elevation of plasma triglyceride concentrations seen following infection of cattle and rabbits with African trypanosomes [1] and upon treatment of rodents with bacterial LPS [2,3]. On the other hand the protein was isolated as "tumor necrosis factor", a mediator responsible for the induction of hemorrhagic tumor necrosis, following the combined challenge with endotoxin and BCG (Bacillus Calmette-Guérin) [4].

To date, it is well accepted that the pleiotropic cytokine is involved in a wide variety of physiological conditions. Endogenous TNF is an important mediator of innate immunity, and has been shown to be essential for the development of a successful response to bacterial infections [5]. Produced at sites of bacterial, fungal, parasitic or viral invasion, it efficiently recruits and activates defence mechanisms. Additionally, under inflammatory conditions, TNF induces the synthesis of pro-inflammatory mediators. Other biological activities influenced by TNF include cell proliferation and differentiation [6], cell death [7,8,9], neuroprotection [10], and neurotransmission [11].

The strength and duration of TNF expression greatly influences the effect of this cytokine. However, inappropriate production may result in pathological conditions. Indeed, the development of endotoxic shock [2,12], cerebral malaria [13], and autoimmune diseases such as rheumatoid arthritis [14,15,16] have been correlated with high systemic levels of TNF. In addition, the sustained generation of this cytokine is associated with multiple organ failure[17], multiple sclerosis [18,19], cardiac dysfunction [20], artherosclerosis [21], ischemia-reperfusion injury [22], insulin resistance [23,24], and inflammatory bowel disease [25]. A more detailed overview of the pleiotropic activities of TNF can be found in recent reviews [26,27].

1.1.1 Synthesis and Structure

TNF is primarily produced by activated macrophages but also by mast cells, endothelial cells, fibroblasts, T-, and B- lymphocytes.

It is synthesised as a proform, a 26 kDa type II transmembrane protein, that is biologically active as a homotrimer [28]. To obtain the soluble form of the cytokine, the precursor has to be cleaved proteolytically by a metalloprotease, the TNF converting enzyme (TACE) [29]. As the result of the cleavage a 17 kDa peptide is generated, that is released in a homotrimeric form [28].

1.1.2 Signal transduction via TNF receptors

The soluble TNF homotrimer has a triangular structure with the receptor binding sites situated at the interface between two neighbouring subunits, implying that every TNF trimer has three interaction sites with its receptors. The ligand-induced cross-linking of the receptors, which can be mimicked by agonistic anti-TNF receptor antibodies [30], leads to signal transduction and therefore to the TNF-receptor mediated effects.

Membrane-bound TNF mediates effects at the local, paracrine level via cell to cell contact [31], whereas soluble TNF acts at longer distances, generating systemic responses to this cytokine.

It is commonly known that TNF exerts its activities by interacting with two distinct TNF receptors with molecular masses of 55 kDa (TNFR1) and 75 kDa (TNFR2), respectively, which are independently expressed on cell surfaces [32,33]. Whereas TNFR1 seems to be constitutively expressed in most tissues, TNFR2 expression is inducible and more restricted. It can be found especially on immune cells but also on cells isolated from endothelial and neuronal tissue [34]. Another difference between these receptors involves their localization within the cell. During steady state conditions, the majority of TNFR1 molecules are found in the perinuclear Golgi-Complex [35], whereas most TNFR2 molecules are expressed on the cell surface.

TNFR2 is a member of the non-death domain-containing subgroup of the TNF receptor family. Upon activation, this receptor type leads to the ubiquitinylation and subsequent degradation of TRAF-2, a factor which inhibits the formation of the death inducing signalling complex (DISC) and which activates the transcription factor

NF-κB. As such, the activation of TNFR2 can increase the TNFR1-mediated induction of apoptosis [36]. TNFR2 appears to affect only a limited number of cellular responses, many of which are restricted to T cell populations and include effects on proliferation, cell viability [37,38] and cytokine production [39]. In many biological systems, TNFR2 plays an accessory role in TNFR1 mediated responses. To some extent, this cooperation has been explained by ligand-passing, a process by which TNF is concentrated near the cell surface by selectively binding to TNFR2 (K_d 100pM), dissociates from the receptor, and subsequently binds with increased efficiency to TNFR-1 (K_d 500pM) [40]. However, recent reports favour alternative explanations, such as the previously mentioned interaction with TRAF-2 [36].

TNFR1 carries a death domain in its cytoplasmic part and therefore represents a direct activator of apoptotic caspases after recruitment of TRADD and FADD. In addition to its cytotoxic activity, TNFR1 is a strong activator of gene induction. Receptor-bound TRADD serves as an assembly platform also for recruitment of TRAF-2 and receptor-interacting protein (RIP) [41], which act together in the activation of the inhibitor of κB kinases, leading to the activation of NF-κB [42].

It has been shown that TNF can induce the release of the extracellular domains of both receptor types in the circulation of mice by proteolytic cleavage [43,44,45]. The biological relevance of this shedding has been described as antagonistic for TNF bioactivity, since soluble TNFRs retain the ability to bind TNF [46-48].

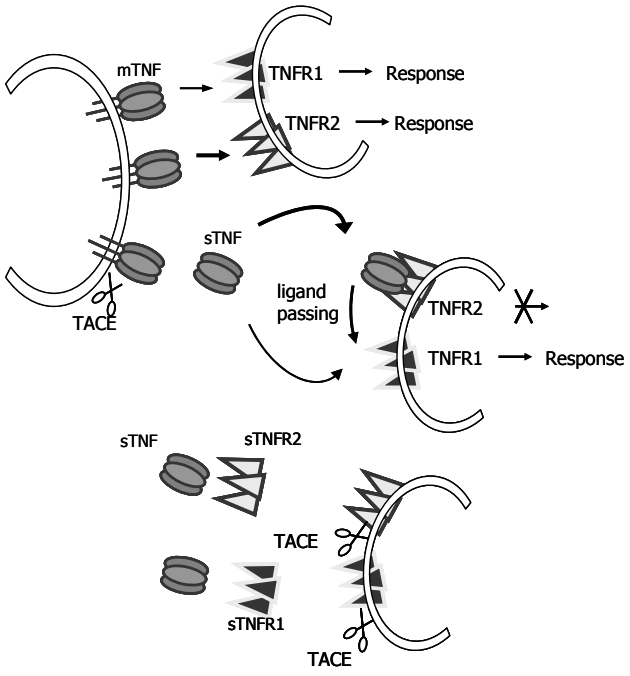

Figure 1.1: Signalling and processing of TNF and its receptors.

1.1.3 The lectin-like domain

In addition to binding to mammalian TNFRs the TNF molecule possesses a lectin-like affinity for chitobiose and trimannoses [49,50] that is located at the extreme top of the TNF trimer, spacially distinct from the receptor binding sites [51]. For soluble TNF it has been shown that this domain is able to bind targets like conserved chitobiose-oligomannose (GlcNAc(2)-Man(5-9)) moieties of the variant surface glycoprotein antigen (VSG) of *African trypanosomes* [52]. This binding leads to the uptake of the cytokine by endocytosis, resulting in a developmentally regulated loss of osmoregulatory capacity and subsequently in the lysis of these parasites [53]. A synthesised, 17-amino acid peptide mimicking the trypanolytic domain of TNF (the tip-peptide) has been shown to be trypanolytic by itself [51]. There are three amino acids within the tip-region that have been proven to be critical for the lectin-like activity. Replacement of Glutamine 107 and 110 as well as Threonine 105 in human TNF and T104, E106 and E109 in mouse TNF leads to a loss of the mentioned trypanolytic activity of TNF. This mutant is called the triple-mutant of TNF [54].

Another interesting effect of the lectin-like domain and also of the tip-peptide is the interaction and regulation of ion channels in several cell types. It has been shown that tip mediates the activation of sodium channels in lung microvascular endothelial cells [55], alveolar epithelial cells [56] and peritoneal macrophages [55]. Since several studies indicate that active salt transport drives reabsorption of edema fluid from the distal airspaces (reviewed by Matthay et al. [57]), the sodium channel activating effect of TNF in type II alveolar epithelial cells could potentially induce fluid clearance from the lung. Indeed it has been shown in an *in vivo* and *in vitro* flooded lung model in rats, that intratracheally administered tip-peptide leads to the activation of fluid reabsorption from the airspaces [58].

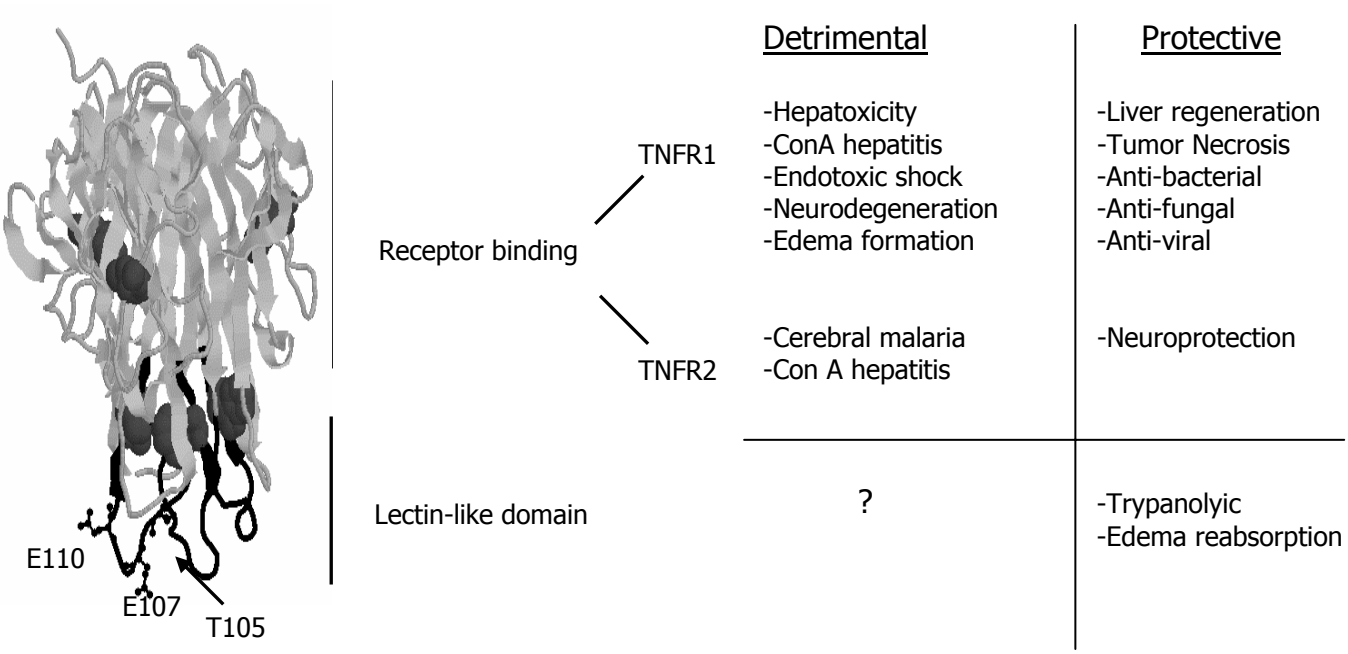

Figure 1.2: Tumor necrosis factor: at least 2 functional domains within one cytokine
(taken from Lucas et al. Current Trends in Immunology, Vol. 4, 2002)

1.2 Pulmonary edema clearance

There is convincing evidence that the vectorial transport of salt and water across the alveolar epithelium is the primary mechanism of fluid clearance (reviewed by Matthay et al. [59]). This transport accounts for the ability of the lung to remove water at the time of birth as well as in the mature lung when pathological conditions lead to the development of pulmonary edema.

The airways and alveoli in the adult human lung constitute the interface between lung parenchyma and the external environment and are lined by continuous epithelium. The distal airway epithelium is composed of terminal respiratory and bronchiolar units with polarized epithelial cells that have the capacity to transport sodium and chloride, including ciliated Clara cells and nonciliated cuboidal cells [60-62]. The alveoli themselves are composed of a thin alveolar epithelium (0.1-0.2 µm) that covers 99% of the airspace surface area in the lung and contains two morphological distinct cell types. The squamous type I alveolar epithelia cells (50-100 µm) cover 95% and the cuboidal type II cells (10 µm) 5% of the alveolar epithelium [63,64]. Both tight junctions [65-67] and gap junctions [68-70] couple type I and type II cells, providing barrier functions and pathways for intercellular communication. Type II cells

synthesize, secrete, and recycle surfactant components and mediate repair to the injured alveolar epithelium. When type I cells are damaged and sloughed from the alveolar surface, type II cells divide, with cell progeny either maintaining morphologic characteristics of type II cells or spreading over the denuded basement membrane and transdifferentiating into type I cells [71].

Active fluid reabsorption can occur in all segments of the pulmonary epithelium. However, since alveolar epithelial cells comprise 99% of the total airway surface, it is likely that the alveolar epithelium plays a predominant role, although the distal bronchiolar epithelium may contribute.

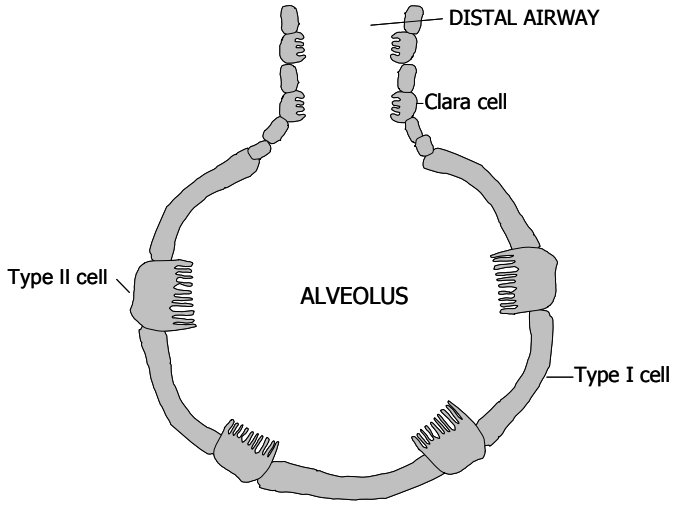

Figure 1.3: A schematic diagram of the pulmonary epithelium (*modified from Matthay et al. Physiological Review Vol. 82, 2002)*

The most extensively studied cell in the distal pulmonary epithelium is the alveolar type II cell, partly because type II cells can be readily isolated from the lung and studied *in vitro*. The alveolar type II cell is responsible for the vectorial transport of sodium from the apical to the basolateral surface [72-77]. This active transport of sodium by type II cells appears to provide a major driving force for removal of fluid from the alveolar space, although the role of the alveolar type I cell remains to be identified.

Na^+ ions enter the apical membranes of alveolar epithelial cells in part through amiloride-sensitive cation channels and are transported across the basolateral membrane by the ouabain-inhibitable Na,K-ATPase [75,78,79]. Na,K-ATPases are transmembrane proteins consisting of α and β subunits. The α-subunit binds and cleaves the high energy phosphate bond of ATP, whereas the β-subunit is apparently responsible for the assembly and normal function of the enzyme complex in the

plasma membrane [80,81]. The Na,K-ATPase works in coordination with the apical Na+ channel to generate an electrochemical gradient which results in a vectorial Na+ flux from the airspace and subsequent iso-osmotic movement of water from the airspaces [78,79] .

In a lot of different species, stimulation of β_2-adrenergic receptors in intact lungs by synthetic agonists (terbutaline, salmeterol, isoproterenol) or endogenous and exogenous epinephrine, respectively, increases fluid clearance *in vivo* and *ex vivo* [82-96]. Moreover, studies in newborn animals showed that endogenously released catecholamines can stimulate fluid clearance in the fetal lung. This effect is completely blocked by unspecific (propranolol) or specific β_2-receptor antagonists (ICI 118,551) [83,88,90,92-94,96]. Treatment with amiloride inhibited the β_2-receptor related stimulation of lung liquid clearance, thus indicating the dependence on sodium transport [92,94,96,97]. There is evidence from several studies that cAMP is the second messenger for the β-adrenergic effects [91,98,99]. As such, the activation of fluid clearance by cAMP has been shown to involve two independent mechanisms: 1) the upregulation of apical sodium conductive mechanisms and 2) the basolateral Na,K-ATPase. Thus, cAMP augmented open channel probability [75,100-103] increased the delivery of ENaC channels and Na,K-ATPase to the apical and basolateral membrane, respectively, and induced the phosphorylation of Na,K-ATPase α-subunits [104-107].

A more detailed overview of lung epithelial fluid transport and the resolution of pulmonary edema can be found in recent reviews [108-111].

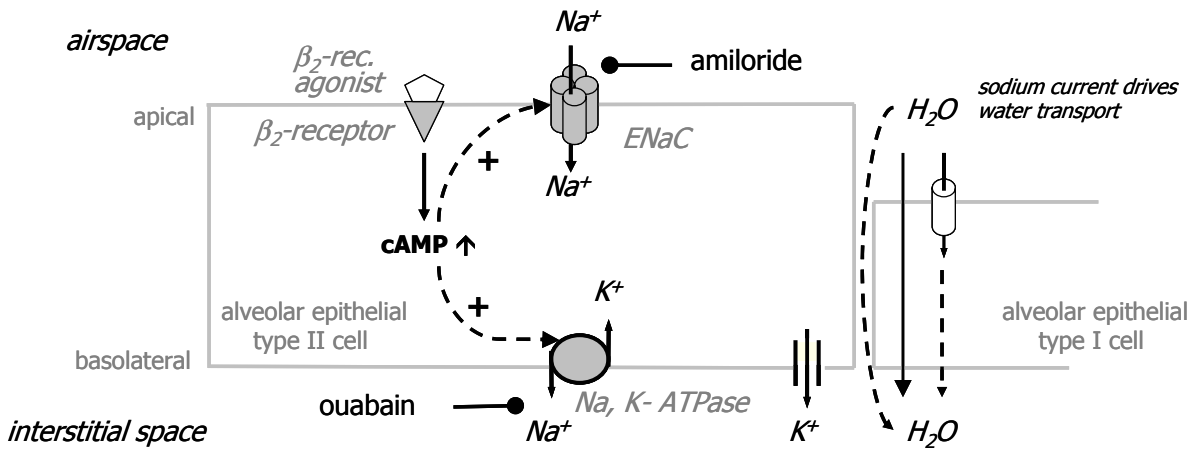

Figure 1.4: Simplified diagram of lung trans-epithelial fluid transport

1.2.1 The dual role of TNF in lung liquid clearance

Several studies [112-116] have demonstrated that TNF may have either a deleterious or a protective effect during the inflammatory response after infectious [117], biological [118], mechanical [119,120], or chemical [102,121,122] stimuli.

Thus, TNF was shown on the one hand to promote lung edema formation by receptor-mediated neutrophil activation and infiltration [123-126]. On the other hand, it was demonstrated under clinically important pathological conditions, such as pneumonia [127] or peritonitis [128], that TNF also stimulates epithelial fluid transport and thus prevents the lung from alveolar flooding. Also exogenous TNF, instilled into the lungs of anaesthetized and ventilated rats increased alveolar liquid reabsorption[56,127]. These TNF-mediated effects were all amiloride-sensitive, meaning that they depended on the activation of Na^+-selective amiloride-sensitive channels. Moreover, the promoting activity of the cytokine on edema reabsorption was independent of β_2-receptor stimulation in all mentioned studies.

Because a triple-mutant TNF lacking the lectin-like activity of the cytokine, failed to induce Na^+ influx in A549 cells, and to stimulate edema reabsorption in rats [56], the beneficial effect of TNF on lung liquid balance seems to be linked to its lectin-like domain. However, in the same study, antagonistic anti-TNFR antibodies abolished the effect of TNF on A549 cells. These results provide direct evidence in these cells for a receptor-dependent effect of TNF. In contrast, patch-clamp experiments with alveolar macrophages isolated from TNFR double-deficient mice revealed that TNF increased Na^+ current independently from the TNF-receptors. Moreover, a peptide mimicking the lectin-like domain with no binding to the two TNFRs, the so-called tip-peptide, triggered increases in membrane conductance [55] and activated fluid transport from the distal airspaces in rats [129]. This tip-mediated effect could be totally blocked with N,N`diacetylchitobiose, which specially binds to the lectin-like domain of TNF and blocks its activity. Furthermore, a peptide mutated in the three amino acids essential for the lectin-like activity of the peptide showed no effect on lung liquid clearance. Moreover, the instillation of TNF into the lungs of ventilated rats resulted in an increase of neutrophil infiltration into the alveolar space, whereas instillation of the tip-peptide did not have such inflammatory consequences [58].

1.3 African Trypanosomiasis

African trypanosomes are extracellular protozoan parasites that are transmitted by the bite of the blood-sucking tsetse fly and cause infections in humans, livestock, and rodents [130]. In sub-Saharan Africa, *Trypanosoma brucei rhodesiense* and *T. brucei gambiense* cause the East and West/Central forms, respectively, of human sleeping sickness (HAT), which is responsible for up to 500,000 deaths/year [131]. In addition, *T. brucei brucei, T. vivax* and *T. congolense* are the causative agents of Nagana, a cattle disease similar to HAT that leads to an estimated total loss of >$1 billion/year in agricultural income [132].

In human sleeping sickness, there are two clinical presentations, namely the early hemolymphatic stage of parasite proliferation in the blood and the lymphatic system, and, as a result of blood-brain barrier penetration, the late meningoencephalitic stage, when the CNS is involved. Although *T. brucei rhodesiense* causes a more acute pathology than *T. b. gambiense*, the disease follows the same progression in both subspecies [133].

1.3.1 African trypanosomes and the host immune system

1.3.1.1 Antigenic variation

Independent of the species, the parasites need to resist the exposure to the immune system of their mammalian host for a long time, implying that a well-equilibrated growth regulation system has to exist, allowing the parasites a sufficient survival time to ensure an effective transmission of the species [53,134]. Such a system involves the variant-specific surface glycoproteins (VSGs) that are distributed over the surface of the trypanosome and are anchored to the outer membrane by a glycosylphosphatidylinositol (GPI) anchor [135]. Ten percent of the entire genome, comprising about 10.000 genes, are thought to encode for the VSGs, providing the molecular basis for the antigenic variation observed in trypanosome infections, since only one of these genes is expressed at any time, the rest being transcriptionally silent [135]. Ten million copies of a single VSG species cover the trypanosome surface, acting as a protective coat for the parasite and preventing access to the underlying plasma membrane for the components of non-specific immune responses [136-138]. The switch of the expression between immunologically distinct VSGs provide antigenic

variation and is supposed to provide protection against VSG-specific immune responses [139]. As a result, the parasite undergoes rapid multiplication in the blood of the host, and the partial control by host B cell responses to VSG produces waves of parasitemia that characterize the disease [140].

1.3.1.2 Role of TNF in trypanosome infections

Different breeds of cattle display differential susceptibility to trypanosomal infections with the indigenous West African N`dama and Muturu cattle being relatively resistant, while European and Zebu breeds are comparatively susceptible [141]. Similarly, different strains of mice also exhibit a spectrum of susceptibilities to trypanosomes. BALB/c mice are susceptible to *T. congolense* [142-144] T*. brucei rhodiense* or T*. b. brucei* [145-147] infection, while C57Bl/6 mice are relatively resistant, as measured by the levels of parasitemia, immunosuppression and survival times. Highly susceptible BALB/c mice infected with 10^3 *T. congolense* die in 8.4±0.5 days after infection, while subtolerant C57Bl/6 mice survive for 163±12 days [143,144]. Although it is generally accepted that the antigenic variation of the VSG is the main immune escape mechanism of African tryanosomiasis [137], it is known that the amount of trypanosomiasis-induced antibodies produced by the host does not directly correlate with its relative resistance. Since several studies suggest that the fatal outcome and severity of trypanosome infection in human [148], cattle, and mice have been linked to the induction of excessive inflammatory responses by the host`s immune system, the relative susceptibility may be decided or at least strongly influenced by the patterns of cytokine responses induced [149].

At the level of infection-associated cytokine secretion, induction of IFNγ and TNF has been extensively documented [150-152]. Since both of these type 1 cytokines are involved in parasite control as well as in host pathology, they have been described to play an important dual role in trypanosomiasis. Indeed, using cytokine-deficient mouse models, it has been suggested, that a type 1 cytokine response contributes to trypanosomiasis control. Correlating with INFγ to be accepted as an important factor in infection-associated T cell suppression in the lymph nodes, IFNγ deficient mice suffer from accelerated parasite growth and exhibit a significantly reduced survival time when infected with African trypanosomes [151].

In TNF-deficient mice, efficient control of peak parasitemia levels is impaired, although infection-associated pathology is strongly reduced and survival time is not shortened [153]. In this case it has been reported, that the effect of TNF on peak parasitemia development could be mediated by the direct trypanolytic effect of the cytokine, that has been investigated *in vitro* [51]. This trypanolytic activity is mediated via the tip-sequence of TNF that is able to specifically recognize the conserved N-linked high-mannose moiety of the trypanosome VSG [51,52].

On the other hand, TNF, induced by the parasite`s VSG-GPI anchor[154,155] plays a crucial role in the severe pathology of experimental mouse trypanosomal infections[137] as well as in sleeping sickness in humans [148] and cattle [156]. Although this role has been corroborated using TNF-deficient mice [153], no correlation was found between pathology and TNF serum levels, neither in patients with HAT [157], nor in experimental murine trypanosomiasis [158]. Additionally, no correlation was found between peak parasitemia control or survival and induction of infection-associated pathology [158].

With regard to this, it is important to stress that TNF, as mentioned before, can signal through two independent receptors and that both extracellular domains of these receptors can be released by proteolytic cleavage [43-45], which results in either antagonistic or agonistic activities for the biological function of TNF [46-48].

Since the infection pattern of TNFR2-deficient, but not of TNFR1-deficient mice resembles the pattern recorded in TNF-deficient mice, it was suggested that infection-associated pathology is mediated via TNFR2 signalling [158]. Additionally, the comparative analysis of two conventional mouse laboratory models for high infection-associated pathology (CeH/HeN and C57Bl/6) and two models for low infection-associated pathology (BALB/c and CBA/Ca) reveals that the shedding of soluble TNFR2 correlates with the inhibition of trypanosomiasis-associated pathology [158].

2. Aims of the study

In addition to its receptor binding sites, the TNF molecule possesses a lectin-like domain that is spatially and functionally different from the interaction sites with the receptors. The capacity of the cytokine to promote lung edema reabsorption and the ability to directly kill the bloodstream forms of *African trypanosomes in vitro* has been linked to this TNF region. A peptide mimicking the tip-domain of the cytokine, the so-called tip-peptide, exerts both activities as well. However, the role of the lectin-like domain within endogenous TNF *in vivo* has not been analysed so far.
Therefore the aims of the present study were:

1) the generation of a triple-mutated k.i. mouse expressing a form of TNF that lacks the lectin-like activity of the cytokine,
2) the development and evaluation of an *in vivo* flooded mouse lung model to study the role of the lectin-like domain in lung liquid clearance,
3) to investigate the role of the lectin-like domain in host-parasite interrelationship during experimental trypanosomal infection.

Because an interaction of the lectin-like domain with the TNF receptors is also indicated from the literature, another objective was to study the involvement of the lectin-like domain in TNFR1/TNFR2 activation of soluble and transmembrane TNF.

3. Materials and Methods

3.1 Materials

3.1.1 Chemicals and reagents

BD Biosciences (Heidelberg, Germany): Bacto agar

Biosource (Camarillo, USA): Alamar blue

Biomol (Hamburg, Germany): Dithiothreitol (DTT)

Boehringer Mannheim GmbH (Mannheim, Germany): fetal calf serum (FCS)

DeltaPharma (Pfullinen, Germany): Ringer`s lactate, isotonic NaCl solution

Gibco BRL Life Technologies (Eggenstein, Germany): Penicillin- Streptomycin

ICN Biomedicals (Ohio, USA): 3-[(3-cholamidopropyl)-dimethylammonio]-1-propanesulfonate (CHAPS), N-2-Hydroxyethylpiperazine-N'-2-ethanesulfonic acid (HEPES)

Innogenetics (Ghent, Belgium): recombinant mouse TNF

Interactiva (Ulm, Germany): oligonucleotides

MBI Fermentas (Vilnius, Lithuania): Lambda-DNA (EcoRI/ HindIII)

Merck (Darmstadt, Germany): β-mercaptoethanol, imidazole

New England Biolabs (Schwalbach, Germany): chitin beads

Riedel de-Haen (Seelze, Germany): Dimethylsulfoxid (DMSO), 2-propanol, ethanol absolute

Roche (Mannheim, Germany): Pefabloc SC,

Roth (Karlsruhe, Germany): Tryptone Peptone (pancreatic digest), yeast extract, Ethylenediaminetetraacetate (EDTA), acrylamide/bisacrylamide (37.5:1) solution

Serva (Heidelberg, Germany): Coomassie brilliant blue R250

Sigma-Aldrich (Deisenhofen, Germany): Isopropyl-β-D-Thiogalactopyranoside (IPTG), Triton X-100, glycine, ampicilline, ethidiumbromide, tetramethylbenzidine (TMB), Heparin, Lipopolysaccharide (LPS), Alsever`s Solution

Serva (Heidelberg, Germany): Albumine bovine Fraction V (BSA)

PAA (Cölbe, Germany): PBS, RPMI, Eagle´s MEM, Trypsin-EDTA, Accutase

PeqLab (Erlangen, Germany): PeqGOLD universal agarose

Uptima (Montlucon, France): Pierce BCA protein assay reagent, EthylGlycol bisSulfoSuccinimidylSuccinate (EGS)

Whatman LTD (Maidstone Kent, England): diaminoethyl cellulose (DEAE)

All standard chemicals were purchased primarily from Sigma-Aldrich (Deisenhofen, Germany)

3.1.2 Laboratory equipment and technical devices

Amicon ultrafiltration devices: (Millipore, Eschborn, Germany)

Blottingapparatus: Bio-Rad Transblot SD semidry transfer cell (Bio-Rad Laboratories GmbH, Munich, Germany)

Cell culture material: culture flasks, plastic pipettes, 96 well plates (Greiner, Frickenhausen, Germany)

Centrifuges: Eppendorf 5417R (Netheler & Hinz, Hamburg, Germany), Beckmann GS-6KR (Beckmann Coulter, Krefeld, Germany), Sorvall RC 28S (Kendro Laboratory Products, Langenselbold, Germany)

Differential pressure transducer: ISOTEC (Hugo Sachs-Elektronik – Havard Apparatus GmbH, March-Hugstetten, Germany)

ELISA Plates: F96 Maxisorp (Nunc, Roskide, Denmark)

Gel-chambers: Novex Xcell II (Novex, SanDiego, USA), Easy Coast (Owl, Portsmouth, USA)

Geldocumentation: Imagemaster VDS (Pharmacia Biotech, Uppsala, Sweden)

Microscopes: Zeiss Televal 31 (Zeiss, Oberkochen, Germany), Leitz SM-Lux (Leitz, Wetzlar, Germany)

PCR cycler: GeneAmp PCR System 2400 (Perkin Elmer, Norwalk, USA)

Photometers: SLT Spektra rainbow photometer (SLT instruments, Crailsheim, Germany), Gene Quant RNA/ DNA Calculator (Pharmacia, Uppsala, Sweden)

Protein purification column: PolyPrep® (BioRad, Munich, Germany)

Sonifier: Sonic Power Company (Dansbury, USA)

Ventilator: HSE-Havard MiniVent 845 (Hugo Sachs-Elektronik – Havard Apparatus GmbH, March-Hugstetten, Germany)

3.1.3 Kits

Machery & Nagel (Düren, Germany): Nucleobond Ax plasmid purification Kit

Quiagen (Hilden, Germany): DNeasy Tissue Kit, MinElute PCR Purification Kit, MinElute Reaction Cleanup Kit

R&D Systems Inc. (Minneapolis, USA): mouseTNF-alpha/TNFSF1A DuoSet ELISA

Stratagene (La Jolla, USA): QuikChange Site-Directed Mutagenesis Kit

3.1.4 Antibodies

Anti-Mouse IgG: Peroxidase-conjugated AffiniPure Donkey (Jackson Immuno Research Laboritories Inc., West Baltimore, USA)

Anti-Mouse IgM: Peroxidase Conjugate F(ab`)$_2$ fragment of Affinity Purified Goat: (Rockland, Gilbertsville, USA)

80M2: Monoclonal kindely provided by Dr. Peter Scheurich (University of Stuttgart, Germany).

3.1.5 Enzymes

3.1.5.1 Restriction Enzymes

The restriction enzymes and the recommended buffers were purchased from: MBI Fermentas (Vilnius, Litauen); New England Biolabs (Schwalbach, Germany).

3.1.5.2 DNA modifying enzymes

New England Biolabs (Schwalbach, Germany): alkaline phosphatase (CIP), T4 DNA ligase

Perkin Elmer (Norwolk, USA): *Pwo* polymerase

3.1.5.3 Further enzymes

Sigma-Aldrich (Steinheim, Germany): lysozyme

3.1.6 Peptides

Human circular tip-peptide: (Innogenetics, Gent, Belgium, and Bacchem, Heidelberg, Germany)

Murine circular tip-peptide: (Bacchem, Heidelberg, Germany and EMC microcollections GmbH Tuebingen, Germany)

3.1.7 Anaesthetica and Drugs

Amiloride: (Sigma, Deisenhofen, Germany)

Diazepam: (Ratiopharm Ulm, Germany)

Kemit: Ketaminehydrochloride (ALVETRA GmbH, Neumünster, Germany)

Narcoren®: sodium pentobarbital (Merial GmbH Ballbergmoos, Germany)

Pancuronium: Pancuronium bromide (Arzneimittel GmbH, Freiburg, Germany)

Propranolol: (Sigma, Deisenhofen, Germany)

Terbutaline: (Sigma, Deisenhofen, Germany)

3.1.8 Cell lines and microorganisms

HepG2 cells, WEHI cells: (DMSZ, Braunschweig, Germany)

MF-R1-Fas cells, MF-R2-Fas cells: kindly provided by Dr. Peter Scheurich (University of Stuttgart, Germany)

***T. brucei brucei* AnTat 1.1E:** kindly provided by Dr. Stefan Magez (University of Brussels, Belgium)

***E.coli* ER 2566:** (New England BioLabs, Schwalbach, Germany)

3.1.9 Mice

Balb/c, and C57Bl/6 (wild type-, triple mutated TNF (B6-TNF$^{tm1.1Blt}$), and TNFR2-deficient (p75$^{-/-}$)) were obtained from the animal facility of the University of Constance (Germany).

C3HHeN were purchased from Charles River (Charles River Wiga Deutschland GmbH, Sulzfeld, Germany)

All animals were bred at the animal facility of the University of Constance. They received human care in accordance to the national animal health guidelines and the legal requirements in Germany. Mice were kept at a temperature of 24°C, 55% humidity, 12 hour light-dark cycles, with regular chow (Altromin C 1310) and water provided *ad libitum*. For the duration of the experiment animals were kept in filter-top cages.

3.2 Methods

3.2.1 Molecular cloning and DNA analysis

3.2.1.1 Polymerase Chain Reaction (PCR)

This highly sensitive method allows the analysis, amplification or, using modified conditions, the mutation of specific segments of DNA. A temperature resistant bacterial DNA-polymerase is used for the amplification of the DNA-matrix starting at specific oligonucleotides. These primers are specifically chosen to flank both ends of the target sequence. The 3`OH ends of the primers are elongated in a complementary manner. By successive cycles of denaturation, annealing of the oligonucleotides to the complementary DNA-segment, and elongation, the target sequence is amplified logarithmically. The yield can be optimized by adapting reaction conditions such as temperature, duration of the cycle steps and cycle number to the demands of the target sequence (thermodynamic stability of the primer-DNA-hybrids, segment size).

For the amplification of DNA sequences required for molecular cloning, the use of a polymerase with an intrinsic proof reading activity such as *Pwo* is recommended.

The reaction mix was prepared by transferring 20 ng of template-DNA (plasmid) into a PCR reaction tube and adding 1 U of DNA Polymerase, 10 µl of each primer (10 µM), 10µl of dNTP solution (2 mM), 10 µl of enzyme specific 10x reaction buffer and H_2O up to 100 µl.

The amplification occurred in a thermo cycler. In a first step the matrix DNA was denatured for 2 min at 95°C, followed by amplification in successive cycles.

Denaturation: 1 min, 95°C

Annealing: 1 min, temperature dependent on primer length and nucleotide composition

Elongation: time adapted to sequence length and enzyme efficiency (efficiency of *Pwo*-polymerase about 500 bp/ min), 72°C

The cycles were repeated 30 to 40 times. At the end of the last cycle a final elongation step of 10 min at 72°C was performed and subsequently the reaction was stopped by cooling to 4°C.

3.2.1.2 Purification of the PCR product

For further cloning steps requiring different buffer conditions (restriction) and for the removal of the DNA polymerase, respectively, the PCR product was purified from the PCR reaction mixture using the PCR purification Kit (Qiagen) according to the user directions.

3.2.1.3 DNA-cleavage with restriction enzymes

Restriction enzymes are DNA hydrolases that recognise specific, palindromic DNA-sequences with a size of about 4 to 8 bp. Because these sequences are highly specific for each individual endonuclease, restriction enzymes can be used either to analyze genomic as well as plasmid DNA or to cleave vectors and inserts (subfragments from vectors, PCR products) for molecular cloning.

Suitable amounts of restriction enzyme (1 U = cleavage of 1 mg λ-DNA/ h) were added to a given amount of DNA and reaction buffer. Subsequently, H_2O was added to obtain the final reaction volume and the probe was incubated at the enzyme-specific temperature.

3.2.1.4 Agarose gel electrophoresis

At constant electric field strength, the electrophoretic movement of linearized DNA is inversely proportional to the decadic logarithm of its molecular weight. The use of DNA length markers as a reference allows the determination of the size of separated DNA-fragments.

The concentration of the agarose gel for optimal chromatographic separation has to be chosen depending on the expected length of the DNA fragment:

30- 200 bp	2,0 %
200- 800 bp	1,5 %
800-1500 bp	1,2 %
1500-4000 bp	1,0 %
> 4000 bp	0,8 %

The agarose gel was covered with TBE buffer (90 mM TRIS, 90 mM boronic acid, 2.5 mM EDTA, pH 8.3) before the DNA samples, supplemented with 5x DNA loading buffer (70% (w/v) Saccharose, 100 mM EDTA, 0.01% bromophenol blue), were

loaded. EcoRI/ HindIII restricted λ-DNA was used as a marker. For separation of the DNA, electric field strength of 5-8 V/cm electrode distance was applied.
After electrophoresis the gel was incubated in ethidiumbromide solution (10 µg/ ml) for about 15 min and surplus ethidiumbromide was removed by washing in TBE. Finally the DNA fragments were detected on a UV screen.

3.2.1.5 Isolation of DNA-fragments from agarose gels

For further cloning steps the piece of gel containing the desired fragment was cut out with a scalpel. The DNA was purified by applying the QIAquick Gel Extraction Kit (Qiagen) according to the manufacturer`s manual.

3.2.1.6 Photometric measurement of DNA concentration

The DNA concentration was determined in TE buffer (10 mM TRIS, 1 mM EDTA, pH 8.0) at a wavelength of 260 nm. For double stranded DNA the extinction of 1.0 corresponds to a concentration of 50 µg/ ml. To determine protein contamination the adsorption at 280 nm was measured. A protein free DNA preparation has a quotient A_{260}/A_{280} of 1.8.

3.2.1.7 Dephosphorylation of the vector

To prevent recirculation of a restricted plasmid the 5` phosphate had to be removed before ligation.
Alkaline phosphatase (1 U) was added to the vector DNA obtained from the gel extraction step and supplemented with 10x enzyme specific reaction buffer and H_2O to a final volume of 20 µl. After incubation at 37°C for 20 min, the enzyme was inactivated by heating as recommended by the manufacturer.

3.2.1.8 Ligation

The catalytic activity of the T4 DNA ligase leads to the formation of a phospho-diesterbond between free 3`-OH and 5`-phosphate ends of double stranded DNA.
For ligation, the insert DNA was added at 3-5 times molar excess to the vector DNA. Suitable amounts of insert were mixed with 50 ng of vector DNA, 10 µl of 2x reaction buffer, 1 µl of rapid T4 DNA Ligase and H_2O up to a reaction volume of 20 µl. Finally, the mixture was incubated for 5 min at 24°C.

3.2.1.9 Transformation of ultra competent DH5α

For transformation of DH5α *E. coli*, 100 µl aliquots of bacteria suspension were gently thawed on ice and then transferred into a polypropylene reaction tube. Following addition of 1.7 µl 2-mercaptoethanol solution (10%) the bacteria were incubated on ice for 10 minutes and carefully shaken every other minute. 10 µl of DNA solution (ligation mixture) were added before the bacteria were heat shocked for 45 seconds in a water-bath at 42°C and allowed to cool down for 2 minutes on ice. After adding 900 µl of prewarmed (37°C) LB-Medium (1% tryptone peptone, 1% NaCl, 0.5% yeast extract, 0.5% 1N NaOH), bacteria were incubated at 37°C for 1h in a shaker. Following centrifugation at 3500 rpm, they were resuspended in 50 µl of medium, and incubated on selective agar plates (1.5% BactoAgar, 0.01% ampicillin) for 16-20 hours at 37°C.

3.2.1.10 Plasmid DNA preparation

3.2.1.10.1 Analytical DNA-preparation ("Miniscreen")

By employing this quick method, the DNA yield is relatively low and contamination with protein and RNA is comparatively high. However, the amount and purity are sufficient for restriction analysis, but not for further molecular techniques.

Colonies of transformed bacteria were picked from selective agar plates with sterile toothpicks, transferred into polypropylene tubes containing 2 ml of selective LB medium (1% tryptone peptone, 1% NaCl, 0.5% yeast extract, 0.5% 1N NaOH, 0.01% ampicillin) and shaken for 12 to 16 h at 37°C.

Following centrifugation of 1.5 ml of the suspension for 1 min at 14,000 rpm and 4°C, the pellet was resuspended in 200 µl STET buffer (50 mM Tris, 50 mM EDTA, 8% (w/v) saccharose, 5% TRITON X100, pH 8.0). To digest the bacterial cell walls, 25 µl of lysozyme solution (10 µg/µl) were added before incubating the cells for 1 min at 95°C. Subsequently, the lysate was cooled on ice for 5 min and centrifugated for 10 min at 14,000 rpm and 4°C. The pellet was removed using a pair of tweezers and the supernatant was mixed with 200 µl of isopropanol. The plasmid DNA was precipitated by centrifugation for 5 min at 14,000 rpm and room temperature. The DNA was resuspended in 200 µl TE/NaCl buffer (10 mM TRIS, 1 mM EDTA, 300 mM NaCl, pH 8.0) and precipitated once more by addition of isopropanol and centrifugation. Finally, the pellet was washed using 500 µl of

70% ethanol, dried, and resuspended in 50 µl H_2O. Total yield of plasmid DNA was about 2 to 10 µg per preparation.

3.2.1.10.2 Preparative isolation of DNA

High amounts of highly pure plasmid DNA were obtained from 100 ml to 500 ml suspensions of bacteria grown in selective LB-medium (1% tryptone peptone, 1% NaCl, 0.5% yeast extract, 0.5% 1N NaOH, 0.01 % ampicillin) to an OD_{600} of 1.5 by ion exchange chromatography applying the Nucleobond AX Plasmid Purification Kit (Machery and Nagel) according to the user manual.

3.2.1.11 QuickChange™ Site-Directed Mutagenesis

The QuickChange™ method allows site-specific mutation in virtually any double-stranded plasmid. The basic procedure utilizes a supercoiled double-stranded DNA vector and two synthetic oligonucleotide primers, carrying the desired mutation. The primers, each complementary to opposite strands of the vector, are extended during temperature cycling by *PfuTurbo* DNA polymerase. Incorporation of the oligonucleotide primers generated a mutated plasmid containing staggered nicks. Following temperature cycling, the product was treated with *Dpn I* that is specific for methylated DNA and was used to digest the parental DNA template and to select for mutation-containing synthesized DNA.

The procedure was performed according to the manufacturer`s instructions.

3.2.2 Generation and analysis of recombinant murine TNF proteins

3.2.2.1 Generation of the proteins using the IMPACT™-CN system

The IMPACT (Intein mediated purification with an affinity chitin-binding Tag) method is a protein purification system which utilizes the inducible self-cleavage activity of a protein splicing element (termed Intein) to separate the target protein from the affinity tag in a single chromatographic step without the use of a protease.

For cloning and expression of the recombinant proteins in *E.coli* the pTYB12 vector, an N-terminal fusion vector in which the N-terminus of the target protein is fused to an Intein tag containing a chitin binding domain, was applied. The pTYB vector contains a T7/*lac* promoter to provide stringent control over fusion gene expression. Additionally, the vector carries its own copy of the *lac I* gene encoding the *lac* repressor. Binding of the *lac* repressor to the *lac* operator sequence immediately

downstream of the T7 promotor suppresses basal expression of the fusion gene in the absence of IPTG induction.

Four recombinant TNF proteins with different modifications were generated using the IMPACT system: (1) wild type TNF, (2) triple-mutated TNF, (3) TNF lacking the receptor binding capacity, and (4) triple-mutated TNF lacking the receptor binding capacity. To this purpose, the coding region of the 17 kDa mature TNF either with or without mutated tip-region was obtained from the vector pBacMam2muTNFwt/ pBacMam2muTNFΔTIP by PCR amplification using the primers TYB_TNF_for (ctt gtc gac ctc aca ctc aga tca tct tct) and TYB_TNF_rev (ctt gaa ttc cct tca cag agc aat gac tcc). These primers provide SalI and EcoRI restriction sites, respectively, that allowed the SalI/EcoRI ligation of the 476 bp PCR products into the multiple cloning region of the plasmid pTYB12 to derive the constructs pTYB12muTNFwt and pTYB12muTNFΔtip. The mutated sequence for the TNF mutants lacking the receptor binding capacity was obtained by substituting the tyrosine[86] encoding nucleotides of the TNF gene locus by nucleotides encoding for a leucine. This mutation was inserted by site directed mutagenesis (3.2.1.11) using the primers TNF/ R°A (cga ttt gct atc tca ctg cag gag aaa gtc aac) and TNF/ R°B (gtt gac ttt ctc ctg cag tga gat agc aaa tcg) and the pTYB12 TNF constructs as the template.

The pBacMam2muTNF vector constructs that served as backbones for the cloning were generated as follows: In a first step the TNF encoding insert (nt position 137-887 according to NCBI: NM 013693) was obtained by reverse transcriptase PCR amplification with genomic murine cDNA as a template. The applied primers bacTNFA-2 (ctg cgg ccg cct ccc tcc aga aaa gac acc at) and bacTNFB (agc cat gga aca ccc att ccc ttc aca gag ca) included NotI and KpnI restriction sites, respectively. The insert was ligated into the NotI/KpnI site of the target vector resulting in the construct pBacMam2muTNFwt. Finally, the wild type tip-region was exchanged by the triple-mutated tip-region by restriction and ligation. The mutated fragment was cut out from the vector pBluescript muTNF/sub (described in 4.2.1.2) by PvuII restriction and ligated into the pBacMam2muTNFwt after PvuII mediated removal of the wt tip-region to derive the construct pBacMam2muTNFΔtip.

3.2.2.1.1 Overexpression of the Intein tagged proteins in E. coli ER2566

For overexpression, respective plasmids were transformed into the *E. coli* ER2566 host strain by heat shock. 500 ml of selective LB-medium (1% tryptone peptone, 1% NaCl, 0.5% yeast extract, 0.5% 1N NaOH, 0.01% ampicillin) were inoculated with 5 ml of an overnight culture of the transformed expression strain. The cells were grown in a shaker to an OD_{600} of 0.5-0.8 at 37°C. With the addition of IPTG to a final concentration of 200 µM the expression of the protein of interest was induced. The cells were incubated for an additional 16h at 16°C, followed by centrifugation for 20 min at 4°C with 5,000 rpm using a GS-3 rotor.

3.2.2.1.2 Purification of the Intein tagged proteins

Purification of the target proteins is achieved via the chitin binding domain of the self-cleavable Intein tag, which allows affinity purification of the fusion precursor on a chitin column. In the presence of thiols such as DTT, the intein undergoes specific self-cleavage which releases the target protein from the chitin-bound intein tag resulting in a single-column purification of the target protein.

Bacterial pellets were resuspended in 40 ml of lysis buffer (20 mM HEPES, 500mM NaCl, 1 mM EDTA, 0.1% Triton X-100, pH 8.0). To prevent degradation of the overexpressed product, Pefabloc was added to a final concentration of 2 mM. After incubation for 30 min on ice cells were mechanically broken by sonification on ice for 10x10 seconds with an output of 5, constant duty cycle and breaks of 10 seconds. The lysate was cleared by centrifugation at 15,000 rpm for 30 min at 4°C using a SS 34 rotor.

The chitin column (5 ml of chitin beads suspension for 1 litre culture) was equilibrated with 5 bed volumes of column buffer (20 mM HEPES, 500 mM NaCl, 1 mM EDTA, pH 8.0) before the lysate was loaded. After the liquid had passed through, the column was washed with 5 bed volumes of column buffer and additionally with 5 bed volumes of GroEL removal buffer (50 mM TRIS, 1 M NaCl, 1 mM EDTA, pH 8.0). Subsequently, thiols mediated cleavage was induced by washing with 3 bed volumes of cleavage buffer (20 mM HEPES, 50 mM NaCl, 1 mM EDTA pH 8.5) containing 50 mM DTT. Then the flow was stopped for on-column cleavage at 16°C for 48h. The protein was eluted with 1 bed volume of DTT-free cleavage buffer.

For protein concentration, ultrafiltration cartridges (10 kDa cut-off) were used. Complete removal of DTT was achieved by pressing solvent through a semi permeable membrane by centrifugation and addition of 2 ml of phosphate buffer for several times.

3.2.2.2 Determination of protein concentration by Edelhoch [159]

Above 275 nm the absorbance of a protein depends on its content of the aromatic amino acids tryptophane, tyrosine, and to lesser extent cysteines (disulfide bonds). For a known sequence, the specific extinction coefficient at 280 nm can be calculated as follows:

$$\varepsilon_{280nm} = 5{,}500 \bullet n_{Trp} + 1{,}490 \bullet n_{Tyr} + 125 \bullet n_{cysteine}\ [M^{-1}\ cm^{-1}]$$

A_{280nm} of the protein was measured in PBS and the concentration calculated by Lambert-Beer as follows:

$$c = E_{280}/\varepsilon_{280} \bullet d\ (17{,}000) \bullet \text{dilution factor}$$

3.2.2.3 SDS PAGE

For SDS gel electrophoresis, samples were boiled after addition of the appropriate amount of 5x sample buffer (62.5 mM TRIS, 5% SDS, 400 µM EDTA, 0.05% bromophenol blue, 50 % glycerine, 150 mM DTT, pH 6.8). Proteins were separated on 12% SDS-polyacrylamide gels (PAGE) and subsequently stained and fixed by incubation of the gel in a solution of 0.002% Coomassie-Brilliant-Blue in 50% H_2O, 40% methanol, 10% acetic acid for 20 min at room temperature. Surplus dye was removed by washing with 10 % acetic acid.

3.2.2.4 Chemical crosslinking

Cross linkers are chemical reagents used to conjugate molecules by the formation of a covalent bound. Sulfo-EGS (EthylGlycol bis(SuccinimidylSuccinate)) reacts with amines via the succinimide group.

The crosslinker (in 100% DMSO), was added in a 5 to 40 molar excess over the protein dissolved in PBS. 5 µg of recombinant protein (murine TNF) were mixed with respective amounts of EGS and PBS up to 50 µl. After incubation for 1 h at room temperature the reaction was stopped using 50 mM Tris buffer (pH 8.0). To check the result, a SDS PAGE was performed as described previously.

3.2.3 Cell based assays

3.2.3.1 Cell culture

HepG2, WEHI and MF-R1-Fas/MF-R2-Fas cells were cultured in RPMI 1640 containing 10% FCS, 100 µg/ml penicillin and 100 U/ml streptomycin in a humidified incubator at 5% CO_2 / 95% air. FCS was inactivated by incubating in a water bath at a temperature of 55° C for 30 minutes prior to addition to the medium. Cells were split twice a week in a ratio of 1:5, using Accutase®. Puromycin A [1 µg/µl] was routinely added once a week to TNFR-1 and TNFR2-Fas expressing mouse fibroblasts.

3.2.3.2 Treatment with TNF

HepG2 and WEHI cells were sensitized with 1 µg/ml ActD 30 minutes before treatment with serial dilutions of soluble TNF. ActD was dissolved in isotonic saline, TNF was diluted in PBS. MF-R1-Fas and MF-R2-Fas cells were TNF treated without ActD sensitization.

3.2.3.3 Cytotoxicity assay

Cytotoxicity was measured by the reduction of the tetrazolium dye Alamar Blue™ by viable cells. The assay was performed according to the manufacturer's instructions. Non-treated cells were used to set the basal level of cytotoxicity (i.e. 0% cytotoxicity), cells lysed with 33% EtOH were used to set its maximum level (i.e. 100% cytotoxicity).

3.2.3.4 Isolation of murine peritoneal macrophages

Eight week old C57Bl/6 mice were anaesthetized by an intravenous injection of sodium pentobarbital (Narcoren®, 10 mg/ml). When the animals were asleep, a peritoneal lavage was performed using 10 ml of ice cold PBS. Cells were extracted from the lavage by centrifugation for 10 min at 1,100 rpm and room temperature. After pellet resuspension in 2 ml RPMI 1640 (10 % FCS, 100 µg/ml penicillin, 100 U/ml streptomycin), the macrophages were counted and adjusted to a concentration of $0.5X10^6$ cells/ml medium. 200 µl of the suspension were added to each well of a 96 well plate. The cells were allowed to adhere to the culture plates over night in a humidified atmosphere at 37°C, 5% CO_2, 40% O_2 and 55% N_2, before

non-adherent cells were removed by washing with PBS. Finally, 100 µl of fresh medium were added to each well.

3.2.3.5 LPS (lipopolysaccharide) treatment

To determine the LPS-mediated TNF response, murine peritoneal macrophages were treated with different amounts of LPS (E. *coli* ; Serotype 0172:B8) and incubated for 6 h in a humidified atmosphere at 37°C, 5% CO_2, 40 % O_2, and 55% N_2. Finally, supernatants were removed and frozen at -80°C. Amounts of murine TNF in the supernatants were measured using the DuoSet® ELISA Development System according to the user manual.

3.2.4 Experimental murine trypanosomiasis

3.2.4.1 Infection of the animals

All experiments were performed with freshly thawed parasites. Infections were initiated with an intraperitoneal injection of 5000 living parasites/mouse. Six to eight-week old either male or female wild type-, triple mutated TNF- (B6-$TNF^{tm1.1Blt}$), and TNF-R2-deficient- ($p75^{-/-}$) C57Bl/6 mice were used.

3.2.4.2 Determination of parasitemia levels and cachexia

Parasitemia levels were determined at intervals of two or three days by microscopic analysis on a blood sample taken from the tip of the tail of each infected animal. To facilitate parasite counting, erythrocytes were lysed by diluting the blood 1:10 in erythrocyte lyses buffer (40 mM NH_4Cl; 10 mM $KHCO_3$, 0.1 mM EDTA). Dependent on parasitemia levels, further dilution steps were performed in PSG. The progression of cachexia was followed by weighting the animals and correlating the current to the initial body weight.

3.2.4.3 Serum analysis

To obtain sera from infected animals, about 100 µl of blood from the tail tip were mixed with 5 µl of Heparin (25 mg/ml) and centrifugated at 4°C for 10 min with 13,000 rpm. The supernatant was stored at -80°C before analysis. During the experiment, serum samples were collected once a week.

3.2.4.4 Determination of serum TNF levels

The TNF content of the serum samples was measured using the DuoSet ELISA Development System according to the user manual.

3.2.4.5 Determination of serum Anti-VSG (Variable Surface Glycoprotein) antibody levels

The purified soluble VSG needed for the anti-VSG antibody titer determination was kindly provided by Dr. Stefan Magez (University of Brussels, Belgium). ELISA plates were coated over night at 4°C with 100µl of 5 µg/ml VSG in PBS. After supernatant removal, 200 µl of 1% BSA in PBS were added and incubated for 1h at room temperature to block unspecific protein binding sites. Subsequently, blocking reagent was removed and the plates were incubated over night at 4°C with 100 µl of serial sera dilutions. Finally, plates were washed 4 times and incubated for 1h at room temperature with 100 µl of specific goat anti-mouse IgM (1 µg/ml) or goat anti-mouse IgG (1 µg/ml) antibodies coupled to peroxidase. After additionally washing 4 times, 100 µl of the peroxidase substrate (TMB) were added. About 30 min later the reaction was stopped by adding 50 µl of 1N H_2SO_4, and the optical density at 450 nm (OD_{450}) was measured.

3.2.5 In vitro trypanolysis assay

3.2.5.1 Isolation of Trypanosomes from C3HHeN mice

For the experiments the *T. brucei brucei* AnTat 1.1E clone, that causes a pleomorphic infection in laboratory rodents, was used.

To obtain sufficient amounts, the parasites were isolated from infected C3HHeN mice at the peak of their parasitemia and separated from RBCs on a DEAE52 cation-exchange column equilibrated at pH 8.0 with PSG (PBS supplemented with 1% glucose). The isolated parasites were stored at -80°C in Alsever`s solution supplemented with 10% glycerol.

3.2.5.2 Trypanolysis assay

To analyse the trypanolytic activity of substances *in vitro*, 10^6 purified bloodstream forms of *T. brucei brucei* per ml in PSG were incubated for 5h at 37° in 96 well plates. Finally, living parasites were counted via light microscopy using a Neubauer counting chamber.

3.2.6 The in vivo flooded mouse lung model

3.2.6.1 Ventilation

Mice were ventilated with 100 % oxygen, a constant tidal volume of 200 µl and a breathing frequency of 120 breaths/min. The pulmonary end-expiratory pressure (PEEP) was set to 5 cm H_20 by connecting the expiratory line of the ventilator to a water trap. In order to circumvent the generation of atelectasis as well as to recrute collapsed lung areas a deep breath was triggered manually every 15 min with a maximal pulmonary inspiratory pressure of 25 cm H_20. Pulmonary pressure was measured with a differential pressure transducer and monitored.

3.2.6.2 Preparation of the instillate

The instillate contained 5% w/v bovine serum albumin dissolved in Ringer`s lactate as well as 10 mg/ 100 ml glucose. Iso-osmolality of normal mouse plasma (340 mOsm) was adjusted using sodium chloride. The pH was adjusted to 7.0. After addition of the testing substances, the desired volume of instillate (15 ml/g body weight) was filled into a syringe and pre-warmed in a water bath (39°C). A sample from each instillate served as individual control for subsequent protein determination.

3.2.6.3 Experimental protocol

Male C57Bl/6 wild type, triple mutated ($TNF^{tm1.1Blt}$) or TNF-R1/R2 double-deficient mice (22-30g) were anesthetized by an intraperitoneal Diazepam (0.25 mg) injection, followed by a Ketamin (5 mg) injection six minutes later. To circumvent deoxygenation, the mice were put into a chamber flooded with 100% of oxygen for about 2 minutes. Once the animals lost their paw reflex, they were weighed and placed supine on a heating plate (41°C). Since hypothermia can reduce the rate of alveolar liquid clearance [160], the mice were covered with an aluminium foil. Subsequently, a tracheotomy was performed and a tracheal cannula was inserted

and fixed with a twine. After 10 min of initial ventilation and another peritoneal injection of pancuronium (100 µg), the instillate (15 µl/ g BW) was delivered from the syringe through the tracheal cannula to both lungs, followed by 1 ml air. The animals were ventilated for additional 60 min and finally, lung fluid samples were obtained by holding the mouse head down and collecting the liquid that was pouring out of the tracheal cannula. Occasionally, this was assisted by gentle pressure on the thorax. Samples were centrifugated for 5 min at 13,000 rpm to separate any kind of cell fraction from the liquid and the supernatants were kept to determine the total protein concentration.

3.2.6.4. Determination of total protein concentration by UV photometrie

The absorption of the protein solution was measured at 280 nm. Protein solutions are often contaminated with nucleic acids, which absorb at 280 nm as well. To correct this error, the adsorption at 260 nm was measured and related to the 280 nm value. The protein concentration was determined as follows:

$c\ [mg/ml] = (1.55 \bullet A_{280}) - (0.76 \bullet A_{260})$

4 Results

4.1 In vitro studies assessing the role of the tip-region in transmembrane TNF-mediated signal transduction

TNF exists both as a transmembrane precursor protein and a soluble cytokine that were shown to have different bioactivities on TNFR2 but not on TNFR1. In the case of soluble TNF there is a hint from the literature that the lectin-deficient triple mutant, in which the three amino acids critical for its lectin-like activity were replaced by alanines, had a significantly reduced TNFR2-mediated bioactivity but maintained TNFR1-mediated bioactivity *in vitro* [54], although the previously used system did not clearly distinguish between the two receptor forms. Moreover, in contrast to TNFR1, which is equally well activated by both soluble TNF and transmembrane TNF, TNFR2 can only be efficiently activated by transmembrane TNF [31]. According to these features, the role of the tip-region in transmembrane TNF-mediated signal transduction has been observed in the following experiments.

4.1.1 Experimental system

In contrast to TNFR1, TNFR2 does not possess a death domain, which has been shown to be essential for TNF-induced cytotoxicity [37]. While TNFR1-mediated effects can easily be observed *in vitro*, for example by performing cytotoxicity assays in cells, the detection of ligand-mediated bioactivity on TNFR2 is for this reason more complicated. Furthermore, it is difficult to discriminate between the biological effects of substances on either of the receptors. Therefore, immortalized murine fibroblasts stably expressing receptor chimeras derived from the extracellular domains of the two human TNF receptors and the intracellular death domain of human Fas (MF-R1-Fas; MF-R2-Fas) were used to study the role of the tip-region in transmembrane TNF mediated signal transduction. These cells were treated with the mature forms of murine TNF (17 kDa) either with or without the mutated region, in combination with the monoclonal antibody 80M2. This antibody is TNFR2-specific and mimics the bioactivity of transmembrane TNF when combined with soluble TNF. The mouse fibroblasts, expressing TNFR1-Fas and TNFR2-Fas, respectively [161], as well as the antibody 80M2 [162] have been described and were kindly provided by Dr. Peter Scheurich (University of Stuttgart, Germany).

Figure 4.1: Schematic representation of TNFR1- and TNFR2-Fas chimeric proteins. The cytoplasmatic domain of Fas was fused to the C-terminus of the transmembrane region of TNFR1.
Adapted from Krippner-Heidenreich et al., The Journal of Biological Chemistry, Vol. 277, 2002

4.1.2 Purification of recombinant TNF-proteins expressed in E.coli

The 17 kDa murine TNF proteins were obtained using the IMPACT^{TM}-CN system (intein mediated purification with an affinity chitin-binding tag).

The overexpression of the proteins in *E. coli* was carried out for 16h at 16°C. As a backbone, the pTYB12muTNFwt and pTYB12muTNFΔTIP vector constructs were used. Each of them provides a 72 kDa either wt or Δtip TNF fusion protein with an N-terminal Intein-Tag.

The intensive band in lane one (figure 4.2) indicates a high expression level of the 72 kDa fusion protein under the applied conditions. Furthermore, the small amount of fusion-protein in the flow-through (lane 2) refers to a high binding efficiency of the protein to the chitin-loaded beads. As expected, the DTT mediated self-cleavage of the Intein-tag resulted in the elution of the 17 kDa target-protein. To check cleavage efficiency, the chitin beads were boiled after cleavage and elution in the presence of SDS and used as a probe (lane 4). The most intensive band at 55 kDa, representing intein alone, points to a very efficient cleavage. Only a negligibly small amount of the fusion protein (72 kDa) remained on the column. Additionally, the small 17 kDa band reveals that most of the target protein has been eluted from the column. Based on the Coomassie stain of the eluate, no additional bands could be detected (lane 3), so that no further purification steps were necessary. Thus, the eluate was subjected to ultrafiltration and the protein concentration adjusted to 1 mg/ml. Overall, 1 mg of protein could be purified from 500 ml bacterial culture.

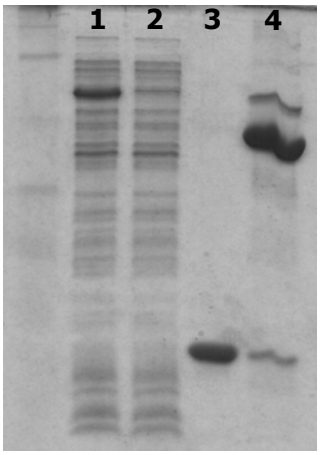

Figure 4.2: Expression and purification of the TNF protein using the IMPACT-CN system.
Lane 1: Clarified crude extract from cells, induced for 16 h at 16°C (load)
Lane 2: Chitin column flow through
Lane 3: Eluate
Lane 4: SDS stripping of remaining proteins bound to chitin column

4.1.3 Bioactivity of the recombinant muTNF proteins in WEHI cells

The bioactivity of the generated 17 kDa TNF proteins was determined by treating WEHI cells with the purified muTNF proteins in the presence of the transcriptional inhibitor Act D (1 µg/ml). It was found that either of the muTNF proteins efficiently induced cell death in WEHI cells. Thus, the EC_{50} values of the IMPACT purified wt muTNF and of a commercial muTNF (His-tag purified) were both about 100 fg/ml (figure 4.3). In contrast the EC_{50} of the triple mutated muTNF was 5 times higher, indicating that this TNF mutant has a reduced capacity to induce cytotoxicity in WEHI cells.

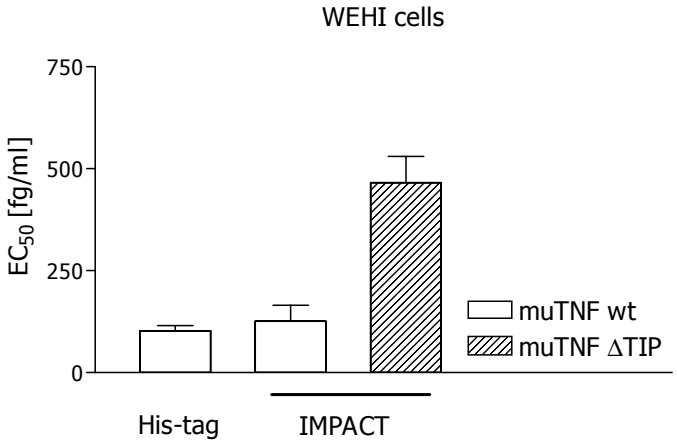

Figure 4.3: Comparison of the EC_{50} values for bioactivity of TNF proteins in WEHI cells after 16h of incubation. Cells were treated with 1 µg/ml ActD 30 min before stimulation.
Data are mean ± SEM.

4.1.4 Trimer formation by chemical cross-linking

It has been reported that correct trimer formation of TNF is obligatory for its bioactivity [163]. To test whether the reduced bioactivity of the mutated TNF in WEHI cells was due to an impaired secondary trimeric structure, the TNF preparations were treated with the chemical crosslinker Sulfo- EthylGlycol-bisSuccinimidylSuccinate (EGS).

As shown in Figure 4.4, EGS treatment resulted in covalent linkage of the TNF subunits. However, no differences in multimer formation could be observed. The cross-linking of wt TNF and triple-mutated TNF, respectively, led to bands corresponding to the monomeric, dimeric, and trimeric forms to the same extent. These results indicate that the mutations in the tip-region do not affect the physiological TNF trimer formation. In conclusion, the reduced ability of the mutated form to induce cell death in WEHI cells can not be attributed to an inhibited interaction of the subunits.

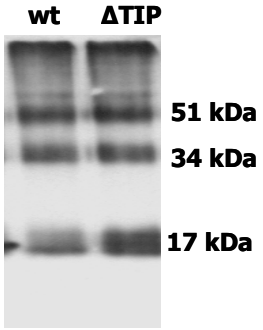

Figure 4.4: TNF trimer formation analysis upon EGS treatment. The assay was performed in a total volume of 50 µl with 5 µg of either wt or Δtip TNF and 50 mM EGS for 1h at room temperature. SDS-PAGE was run with 20 µl of sample and Coomassie stained.

4.1.5 Cytotoxicity of the recombinant muTNF proteins in HepG2 cells

It is commonly known that stimuli induced responses may vary between different cell lines. This can be attributed to differing enzyme or surface receptor settings. For example, it has been reported that HepG2 cells exclusively express TNFR1 [164]. In this context it should be stressed again, that there are hints from the literature for a reduced TNFR2 mediated activity of soluble triple-mutated TNF [54]. Therefore, muTNF wt and Δtip mediated cytotoxicity were additionally tested in absence of TNFR2 on HepG2 cells.

As in WEHI cells either of the TNF proteins induced cell death even in HepG2 cells. However, the EC_{50} values of the His-tagged TNF and the triple mutated IMPACT purified TNF were on the same level in this cell line (Fig 4.5). In contrast, the EC_{50} value of the IMPACT triple mutated TNF was on average 2 times higher. Accordingly, the mutated TNF protein turned out to be even more potent on HepG2 cells than the wt TNF protein. Thus, the inserted mutations did not reduce TNFR1 mediated cell death on HepG2 cells. In conclusion, this experiment together with the cytotoxicity assay in WEHI cells points towards a receptor-type dependent involvement of the

lectin-like domain of TNF in signal transduction that was further investigated in the following experiments.

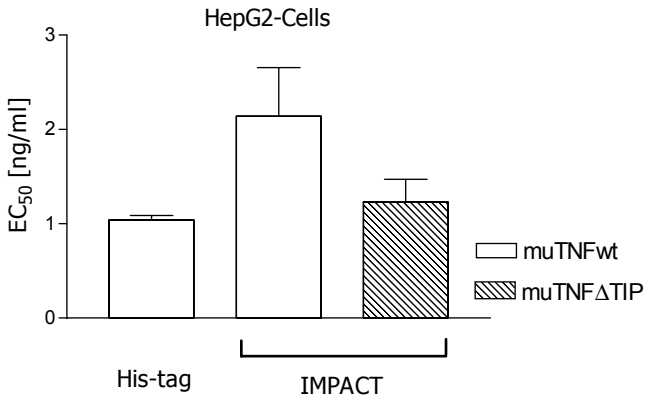

Figure 4.5: Comparison of the EC_{50} values for bioactivity of TNF proteins in HepG2 cells after 16h of incubation. Cells were treated with 1 µg/ml ActD 30 min pre-stimulation. Data are mean ± SEM.

4.1.6 Cytotoxicity of the recombinant muTNF proteins in MF-R1-Fas and MF-R2-Fas cells

To investigate the functional role of the tip-region in transmembrane TNF mediated signal transduction, MF-R1-Fas and MF-R2-Fas cells were incubated with the muTNF proteins in combination with the TNFR2 specific antibody 80M2. The treatment of MF-R1-Fas cells with serial dilutions of either of the different soluble TNF molecules resulted in a strong cytotoxic response with the EC_{50} values of both wt TNF proteins and the triple-mutated TNF protein being nearly at the same level (figure 4.6). Due to its TNFR2 specificity, the addition of 80M2 did not show any effect, as expected. These results further strengthen the hypothesis that the inserted mutations of the TNF tip-region do not affect TNFR1 mediated bioactivity in this model. Accordingly, the tip-region is not involved in soluble TNF/TNFR1 induced signal induction.

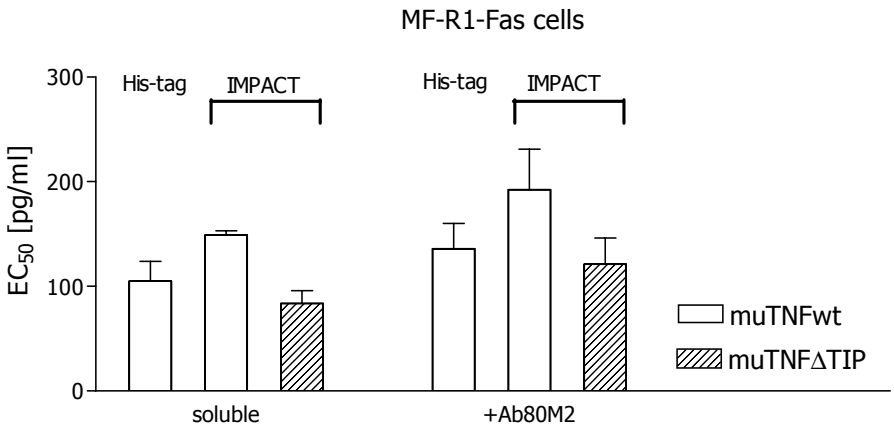

Figure 4.6: Comparison of the EC_{50} values for bioactivity of TNF proteins in MF-R1-Fas cells after 16h of incubation. For costimulation with the antibody 80M2 cells were preincubated with 2 µg/ml 80M2 for 30 min. Data are mean ± SEM.

In contrast to the findings on MF-R1-Fas cells, only a slight cytotoxic effect could be observed on MF-R2-Fas cells when treated with soluble TNF up to concentrations of 100 ng/ml (figure 4.7). This observation correlates with the published finding that TNFR2 can only be efficiently activated by transmembrane TNF [31].

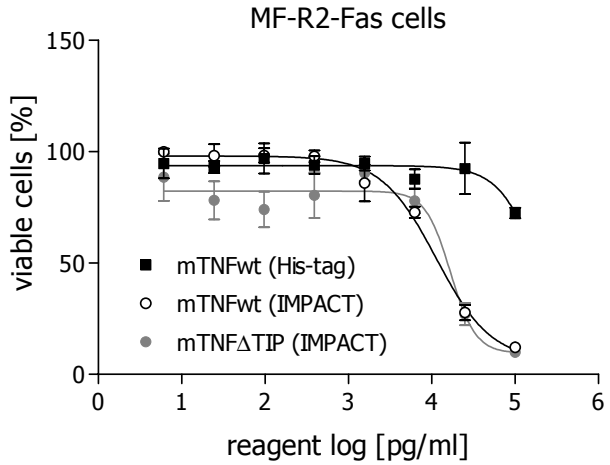

Figure 4.7: Comparison of the EC_{50} values for bioactivity of soluble TNF proteins on MF-R2-Fas cells after 16h of incubation. Data are mean ± SEM.

In the presence of the antibody 80M2, however, a strong cytotoxic response was observed for the wt muTNF protein. In contrast, the cytotoxicity induced by the triple mutated muTNF was reduced about 5-fold (figure 4.8). Based on these results, the conclusion can be drawn that the lectin-like domain of TNF is in fact involved in transmembrane TNF mediated signal transduction of TNFR2.

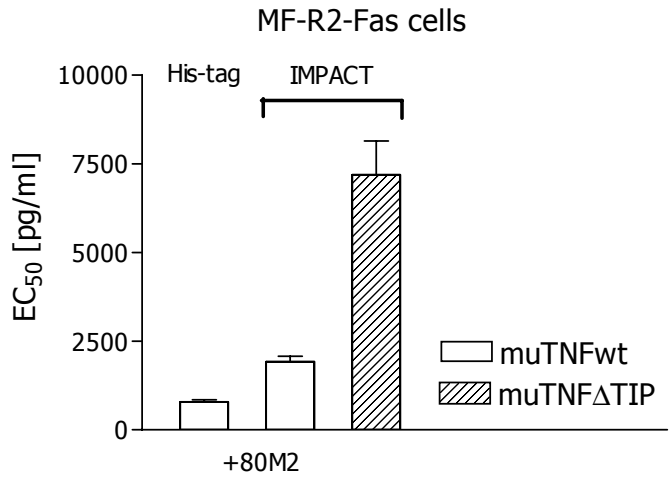

Figure 4.8: Comparison of the EC_{50} values for bioactivity of TNF proteins in MF-R2-Fas cells after 16h of incubation. For costimulation with the antibody 80M2 cells were preincubated with 2 µg/ml 80M2 for 30 min. Data are mean ± SEM.

4.2 Generation of a triple-mutant muTNF knock-in-mouse (B6-TNF$^{TM1.1Blt}$)

This chapter reports the generation of a C57Bl/6 triple-mutant muTNF-knock-in-mouse that has been used as a tool to investigate the role of the TNF tip-region *in vivo* under normal and pathological conditions.

The mutated sequence for the k.i. mouse was obtained by substituting the threonine^{104}-, glutamine^{106}-, and glutamine^{109}- encoding nucleotides of the TNF gene locus by nucleotides encoding for alanines.

4.2.1 Construction of the targeting vector

4.2.1.1 Murine C57BL/6 hybridization library screening

To isolate the genomic TNF gene fragment, a hybridization probe with a size of 300 bp (6203-6484) was generated by PCR amplification using the primers mTNF5`(atc ggt acc tta cac ggc gat ctt tcc gcc c)/mTNF3`(atc ggt acc tta cac ggc gat ctt tcc gcc c), and genomic mouse DNA as the template. Subsequently a C57BL/6 hybridization library screening was performed by Incyte Genomics, Inc. (St. Louis, MO).

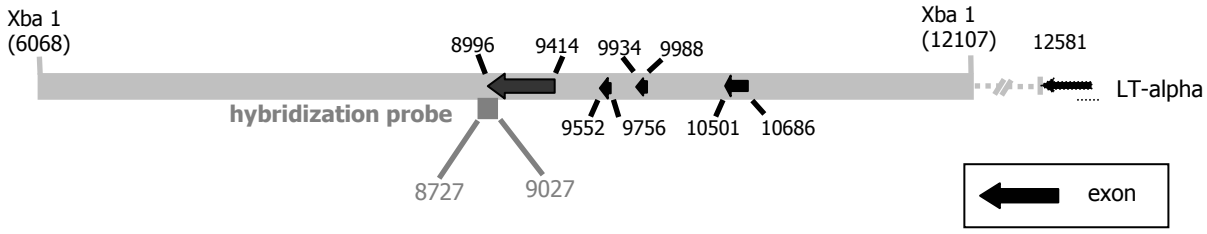

Figure 4.9: TNF gene locus (NCBI: U06950); Hybridazation site of the hybridization probe

As a result of the Bac library screening, three different clones could be identified, each carrying an inserted fragment of about 40 kbp in size, cloned into the pBeloBAC11 plasmid. To check the obtained clones for the TNF gene locus and to isolate the relevant fragment for homologous recombination, the clones were characterized by restriction analysis. Based on the published sequence of the murine TNF gene locus (NCBI: U06950), an XbaI cleavage was expected to result in a

fragment of 6039 bp, including the whole TNF coding region (1650 bp) approximately in the center of the sequence.

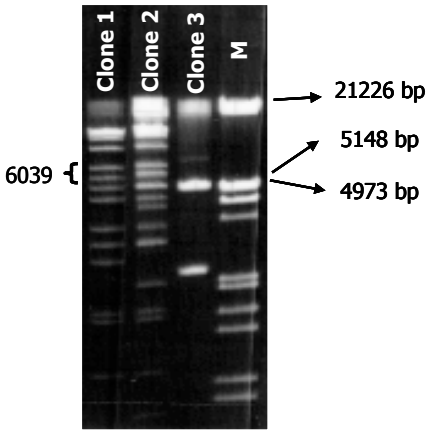

Figure 4.10: Identification of pBeloBAC11 clones by XbaI restriction analysis.

As shown in figure 4.10, the Xba I restriction pattern of clone 1 and clone 2 points to two fragments of the correct size, whereas restriction of clone 3 did not reveal any relevant fragments. Both appropriate fragments were cut from the gel and XbaI cloned into the pGL3-basic plasmid. The following identification of the cloned fragments revealed a pGL3-basic vector construct which contained the relevant 6 kbp segment including the TNF gene flanked by neighbouring sequences.

4.2.1.2 Site-directed mutagenesis

For a better efficiency of the mutation procedure, a smaller PstI/HindIII fragment (figure 4.11, nt 7983-9844), enclosing the tip-region that is located in the first and biggest exon, was subcloned into pBluescript II KS (Stratagene) resulting in the construct pBluescript muTNF/sub.

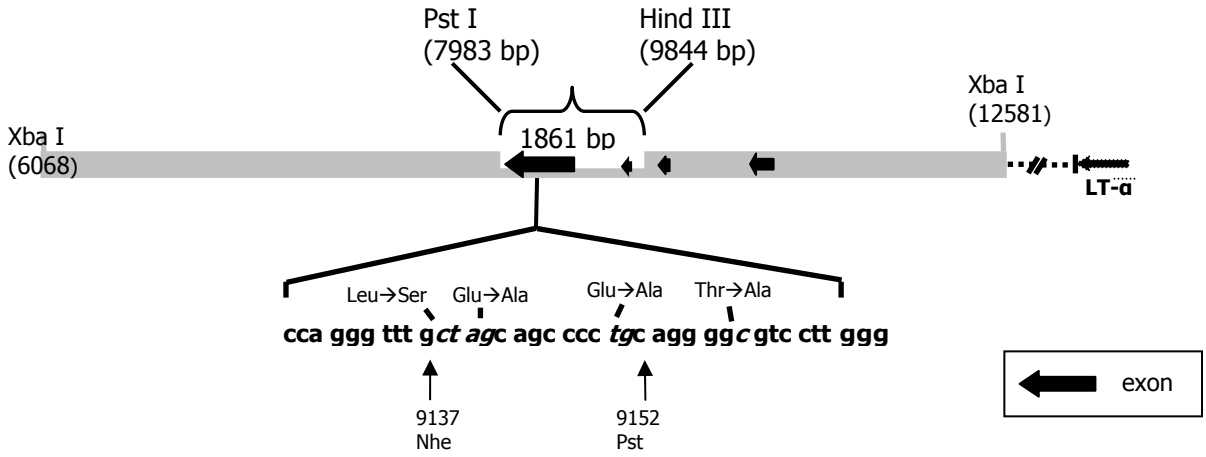

Figure 4.11: TNF gene locus (NCBI: U06950); position and size of the subfragment for site directed mutagenesis

Using the Quick Change Site-directed mutagenesis kit and the primers listed below, the desired point mutations were inserted. The oligonucleotides were adapted to the according sequence changes in each step.

Name	Position	Size	Sequence	AA change
5`mutTNF1	nt 9124-9149	25 mer	gcc cca agg acG CCc ctg agg ggg c	Thr^{104}→Ala
5`mutTNF2	nt 9112-9149	37 mer	gcc cca agg acg ccc ctG CAg ggg ctg agc tca aac c	Glu^{107}→Ala
5`mutTNF3 (2)	nt 9121-9162	41 mer	gct cat acc agg gtt tGC TAg cag ccc ctg cag ggg cgt cc	Glu^{109}→Ala Leu^{110}→Ser

For the molecular characterization of positive ES cell clones, a leucine substitution, Leu^{110}→ Ser was inserted in the third round of mutation leading to the generation of an additional NheI restriction site. The obtained modified PstI/HindIII fragment was finally reintegrated into the native TNF sequence.

4.2.1.3 Insertion of a neo/TK selection cassette

For selection of transformed mouse embryonic stem cells, a neomycin resistance/thymidine kinase selection cassette was inserted into the mutated TNF construct. Briefly, the sequence of the selection cassette flanked by loxP sites was isolated from the pBluesciptSK+ -neo/TK floxed vector construct and integrated into an intron region of the TNF gene at nucleotide position 9552.

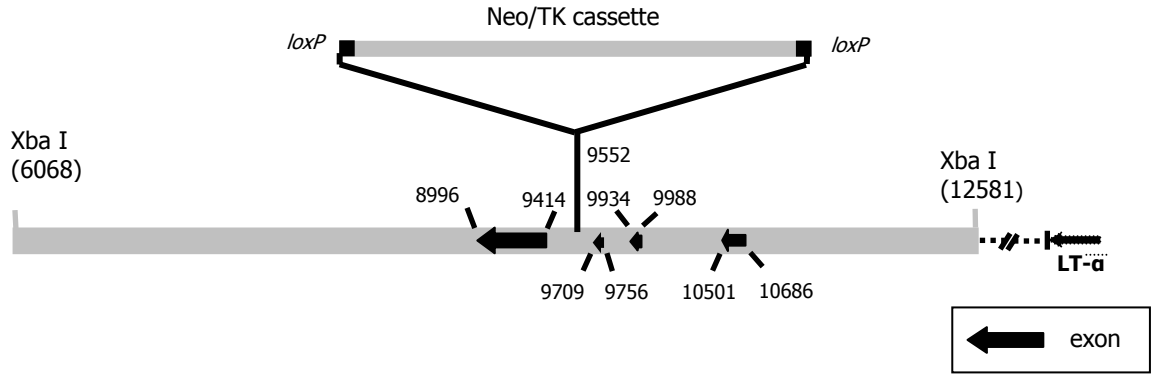

Figure 4.12: TNF gene locus (NCBI: U06950); insertion of the Neo/TK selection cassette.

4.2.1.4 Integration of the triple-mutated target gene into the genome of C57Bl/6 mice

The sequence of operations that finally led to the integration of the triple-mutated gene into the genome of C57Bl/6 mice was performed in the laboratories of Prof. Dr. Horst Bluethman at the Roche Centre of Medical Genomics. This section gives a short overview of the performed procedures.

In a first step, the targeting vector was introduced into a culture of embryonic stem cells (derived from the C57Bl/6 strain) by electroporation. Those cells in which the mutated gene, including the Neo/TK selection cassette, has become integrated into the genome by homologous recombination were selected for resistance to the neomycin-like drug G418. As a result of the selection, 14 mutated clones out of a total of 192 could be identified. These cells were transfected with the Cre recombinase, an enzyme that recognizes loxP sites and excises the intervening DNA. Thus, the Cre/lox recombination led to the removal of the selection cassette from the mutated gene.

In a next step, the cells were injected into mouse blastocysts, which were re-implanted into the uterus of foster mothers. Altogether 27 chimeric mice were born. Out of these, 5 animals (4 female, 1 male) were intercrossed with C57Bl/6 mice. As demonstrated by genotyping, the first generation of offspring from the chimeric animals included heterozygous individuals for the mutated gene, implying that the ES cells entered the germ line of the chimeric animals. Eight of these heteroygous animals were transferred to the animal facility of the University of Constance for further breeding.

4.2.2 Genotyping of the offspring

Complete genomic DNA from the tail tip, extracted by using the DNA easy Tissue Kit (Qiagen) was employed to genotype the offspring by PCR. As a result of the previous cre-lox recombination, one loxP site with a size of 128 bp remained in the TNF gene locus of recombinant mice. Therefore, the primers TNF-945c (tag ttc aca ctc cac atc ctg ag)/ TNF-7nc (caa gcc tgt agc cca cgt cg) spanning this region were used for the genotyping. In the case of wt mice the PCR reaction results in a fragment of 277 bp whereas the fragment received from homozygous k.i. mice had a size of 405 bp. Because the heterozygous animals possess a copy of the wt TNF gene locus as well

as a copy of the mutated TNF gene locus both of the fragments are amplified from their genomic DNA.

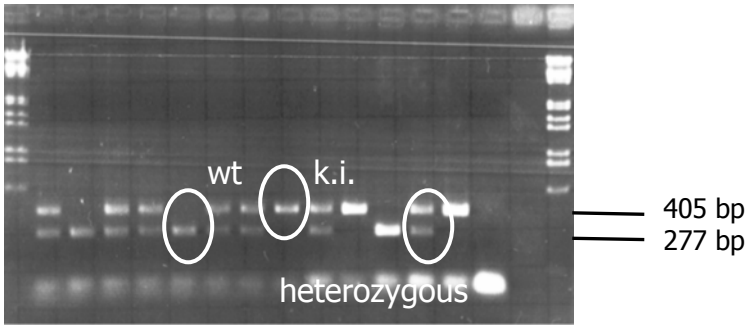

Figure 4.13: Genotyping of the offspring by specific PCR amplification.

A representative result of a genotyping is shown in figure 4.13. As indicated by different fragment patterns, all of the three genotypes could be detected. Statistically, the mutation was passed to the outcome according to the prediction of Mendel`s law. Therefore the modifications of the TNF coding sequence did not turn out to be lethal.

4.2.3 Characterization of the LPS induced TNF response in triple mutated k.i. mice

Modifications of the TNF coding sequence result in an altered primary protein sequence. These alterations may cause dramatic changes in the protein expression level as compared to the wt protein. Accordingly, it had to be investigated whether the k.i. mice were able to produce comparable amounts of TNF upon a stimulus as their wt counterparts. As an experimental system the LPS model was chosen. In figure 4.14 the TNF serum levels of wt mice and triple mutated k.i. mice after 1.5 h of LPS stimulation are illustrated. Although significantly less TNF could be detected in the serum of k.i. mice than in the serum of wt mice, the k.i. mice were in fact able to produce physiologically relevant amounts of TNF upon LPS treatment.

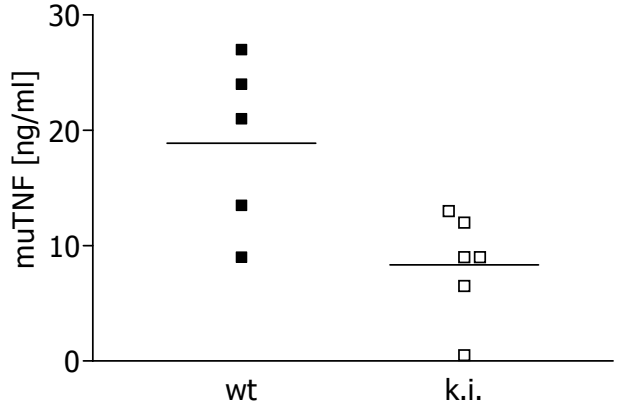

Figure 4.14: TNF level in the serum of C57Bl/6 wt (closed squares) and k.i. mice (open squares) upon intraperitoneal LPS [5 mg/kg] treatment for 1.5 h. The lines indicate the means of the individual values.

These findings were confirmed *in vitro*. As shown in figure 4.15, LPS treatment of peritoneal macrophages isolated from wt and from k.i. mice, respectively, resulted in soluble TNF secretion on a comparable level. This secretion turned out to be concentration-dependent with a half maximum effect of 9 µg LPS /ml in wt, and 7.5 µg LPS /ml in k.i. mice. In contrast to the *in vivo* results, secretion of triple mutated TNF was slightly, but not significantly reduced as compared to wt TNF.

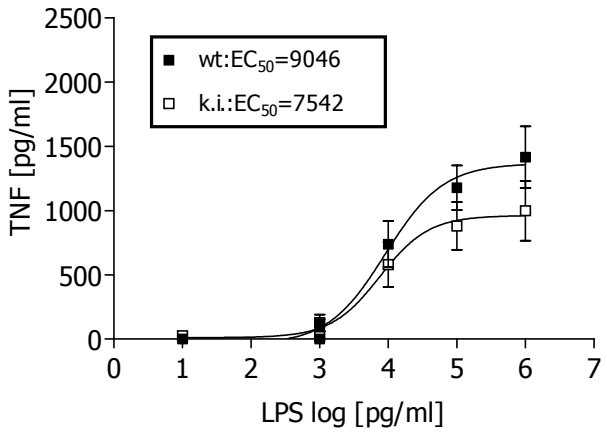

Figure 4.15: TNF response of isolated peritoneal macrophages upon LPS treatment for 6h.
Open squares: macrophages isolated from wild type mice (n=9)
Closed squares: macrophages isolated from k.i. mice (n=9)
Data are mean ±SEM.

In summary, the *in vivo* and *in vitro* results point to a slight influence of the inserted mutations on the secretion of mutated-TNF. However, the gene expression is not prevented and leads to physiologically relevant concentrations of the triple-mutated TNF.

4.3 The *in vivo* flooded lung model

It has been shown that the tip-peptide, that mimics the lectin-like domain of TNF, exerts the sodium transport activating effect of TNF in mammalian cells [165]. Additionally, a lectin-deficient triple mutant of muTNF was reported to lack the cytokine mediated edema absorption effect in an *in vivo* rat model and the Na^+ current activating effect on A549 cells [166]. Recent studies revealed that a circular human tip-peptide increased the lung liquid clearance in an *in vivo* flooded rat lung model, an effect that could be totally blocked with the lectin-binding sugar N,N`diacetylchitobiose, which specifically binds to the lectin-like domain of TNF [129].

To elucidate the role of the TNF tip-region in pulmonary edema absorption, the generated triple mutant muTNF k.i. mice were included in the studies. To this purpose, a suitable mouse model with a clinically relevant setting, the *in vivo* flooded mouse lung model, was established for the following experiments. In this model, pulmonary edema is artificially generated by flooding the lung. Although this is not a clinical edema, it resembles a severe, hydrostatic pulmonary edema in two important points: first, epithelial and endothelial barriers are intact, despite of the liquid, and second, the animal would suffer from a life-threatening hypoxia if not ventilated with exogenous oxygen.

4.3.1 Validation

It has already been reported that $ß_2$-receptor activation stimulates lung liquid clearance [94,167]. However, the postulated tip mediated effects on edema reabsorption have been described to be β_2-receptor independent [129]. Furthermore, combined treatment with the β_2-adrenergic agonist terbutaline and the tip-peptide showed no synergistic or additive effect, indicating a common pathway in the signal transduction of both substances [129]. Hence, it was important to evaluate the basic experimental conditions of the mouse model, regarding stress-induced $ß_2$-receptor stimulation. To that purpose the β_2-antagonist propranolol has been tested in the current model.

As indicated in figure 4.16, non-treated animals, as well as propranolol-treated animals showed a relative reabsorption of 30% on average, implying that propranolol did not significantly affect lung liquid clearance. Thus, a basal stimulation of β_2-adrenergic receptors could be clearly excluded for the applied experimental setting.

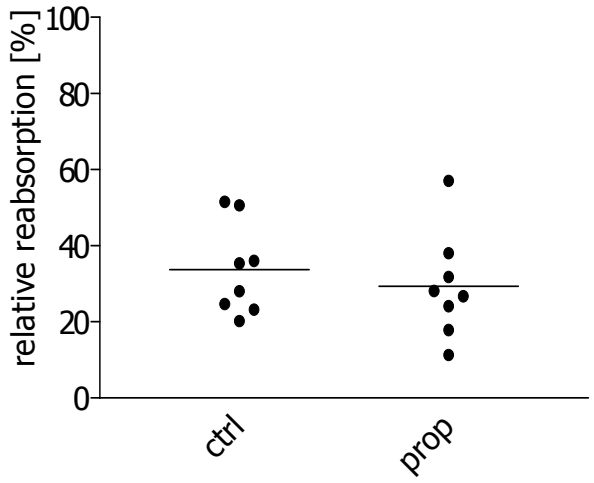

Figure 4.16: Relative edema reabsorption in C57Bl/6 mice, 60 min after instillation of 15 µl/g BW ringer lactate with 5% BSA containing either: ctrl: ringer lactate; prop: propranolol 10^{-4}M. The lines represent the means of the individual values.

Since β_2-stimulation has the capacity to increase fluid clearance, the β_2-agonist terbutaline was used as a positive control to set up the experimental conditions of the *in vivo* flooded mouse lung model. Therefore, mice were treated with buffer alone (ctrl.) or with terbutaline, respectively. To determine the most suitable duration of ventilation, mice were ventilated for different time periods.

After 30 min of ventilation, terbutaline treatment resulted in a slightly, however not significantly increased lung liquid clearance, as compared to controls (figure 4.17). Despite of individual variations between the animals within one experimental group, the β_2-mediated effect proved to be significant after 60 min of ventilation. According to these results the ventilation time was set to 60 min for following experiments.

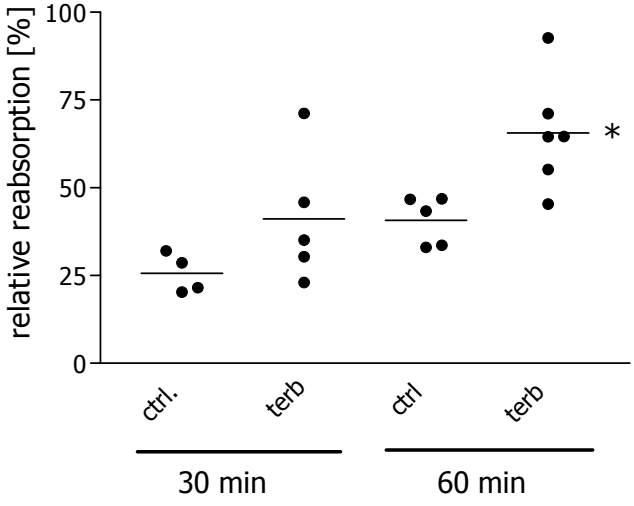

Figure 4.17: Relative edema reabsorption 30 and 60 min after instillation of 15 µl/g BW ringer lactate with 5% BSA containing either: ctrl: ringer lactate; terb: terbutaline 10^{-4} M.
The lines represent the means of the individual values. Unpaired t-test, two-tailed: $p<0.05$ for $ctrl_{60min}$ vs $terb_{60min}$.

4.3.2 Effect of the tip-peptide on lung liquid clearance

Although the human tip-peptide was reported to induce edema reabsorption in an *in vivo* flooded rat lung model, the fluid reabsorption capacity of this peptide still has to be shown in the mouse model. To this purpose, murine tip as well as human tip was tested in C57Bl/6- and in BALB/c mice, using a dose of 12.5 µg and 60 µg per mouse, respectively.

In contrast to terbutaline, neither human nor murine tip-peptide had a significant effect on pulmonary edema reabsorption in the current model (figures 4.18 and 4.19). Because the results were similar in C57BL/6 as well as in BALB/c mice, there is no indication for a strain-dependent effect. Furthermore, different peptide charges from different companies were tested (data not shown). The obtained results did not point to any significant tip-mediated influence on lung liquid clearance.

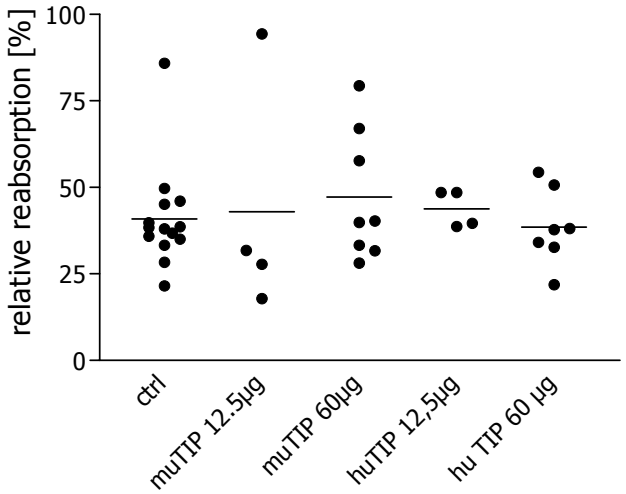

Figure 4.18: Relative edema reabsorption in **C57Bl/6** mice 60 min after instillation of 15 µl/g BW ringer lactate with 5% BSA containing either: ringer lactate (ctrl), muTIP 12.5 µg, muTIP 60 µg, huTIP 12.5 µg, huTIP 60µg. The lines represent the means of the individual values.

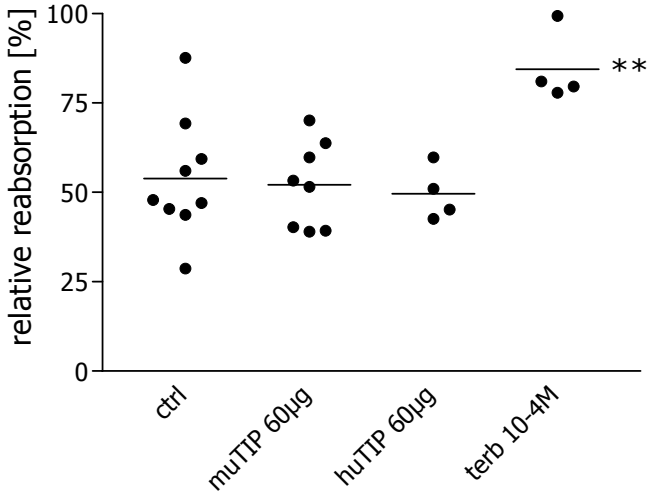

Figure 4.19: Relative liquid reabsorption in **BALB/c** mice 60 min after instillation of 15 µl/g BW ringer lactate with 5% BSA containing either: ringer lactate (ctrl), muTIP 60 µg, huTIP 60µg. The lines represent the means of the individual values. Unpaired t-test, two-tailed: ** $p<0.01$ for ctrl vs Terb.

4.3.3 Ventilation-induced intrapulmonary TNF secretion

Although ventilatory support is an indispensable tool in the treatment of critically ill patients, it is well documented that mechanical ventilation produces or worsens lung injury [168]-[169,170]. Different studies in the literature have indicated a significant correlation between a pulmonary inflammatory response and the development of ventilator-induced lung injury (VILI). In the presence of underlying lung injury, most animal and clinical studies agree that mechanical ventilation exacerbates pulmonary inflammation and injury [171-176]. Such inflammation in the lungs appears to be mediated by proinflammatory cytokines, particularly TNF [177,178]. Additionally, it has been published recently that even in the absence of underlying injury, high tidal volume ventilation (34.5 ml/kg BW) induces intrapulmonary TNF expression in mice[179]. The published high tidal volume of 34.5 ml/kg BW corresponds in mice to a tidal volume of 800 µl. Although in the current model mice were ventilated only with a volume of 200 µl, an additional volume of about 400 µl was instillated. To investigate whether the summed volume of 600 µl could result in the induction of intrapulmonary TNF expression, TNF levels were determined after 60 min of ventilation in the residual lung liquid of C57Bl/6 wt- and of triple-mutated k.i.- mice, respectively.

As shown in figure 4.20, TNF could be detected in the residual lung liquid, indicating a secretion of this cytokine caused by the experimental conditions. On the one hand, the measured concentrations of about 5 ng/ml were equal in both mouse strains, excluding a selective influence of the basally secreted TNF on one experimental group. On the other hand, these observations raised the question whether the amount of the basally produced TNF is able to affect lung liquid clearance via a TNF receptor-dependent effect on ion transport, eventually interfering with the clearance effect caused by treatment with exogenous tip-peptide. The following experiments addressed this question by using a TNF receptor-deficient mouse strain.

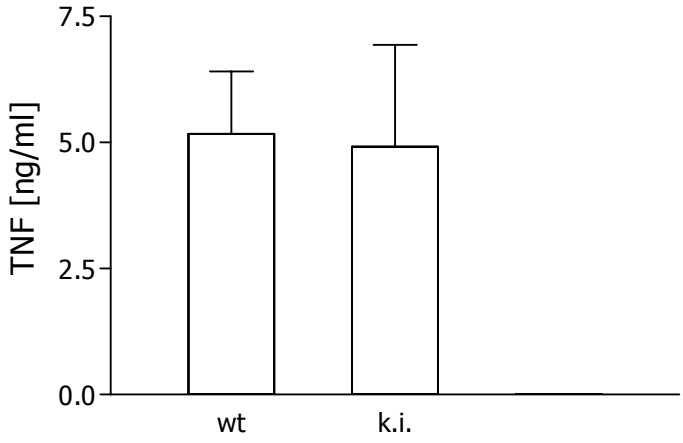

Figure 4.20: Ventilation-induced intra-pulmonary TNF expression in C57Bl/6 wt- and triple-mutated k.i.- mice 60 min after the instillation of 15 µl/g BW ringer lactate with 5% BSA. Data are mean ± SEM. wt: n=6; k.i.: n=7

4.3.4 Influence of basally produced TNF on fluid reabsorption

To investigate the outcome of TNFR-induced effects of the basally produced TNF on lung liquid clearance, the basal level of edema reabsorption after 60 min of ventilation was determined in TNFR1/TNFR2 double deficient mice. Furthermore, in these mice the effect of the tip-peptide, that was described to act independently of either TNFR, was observed.

As shown in figure 4.21 the basal liquid reabsorption was significantly reduced from 32% in wt mice to 21% in TNFR1/TNFR2 double deficient mice. Actually, this reduction points to a TNFR-dependent effect of the basally produced TNF in the flooded mouse lung model. Moreover, the results reveal that the reduced basal reabsorption level observed in TNFR1/TNFR2 k.o. mice could not be significantly abrogated by tip.

Taken together, a reduced basal liquid clearance was detected in TNFR1/TNFR2 double deficient animals, pointing towards a TNFR-dependent effect of the basally produced TNF on lung liquid clearance in the flooded lung mouse model. Even in these mice, lacking the TNFR-mediated effects of the basally produced TNF, treatment with tip could not significantly increase fluid reabsorption however. Hence, there was no indication for a TNF receptor-independent action of the peptide interfering with receptor-dependent actions of endogenous TNF.

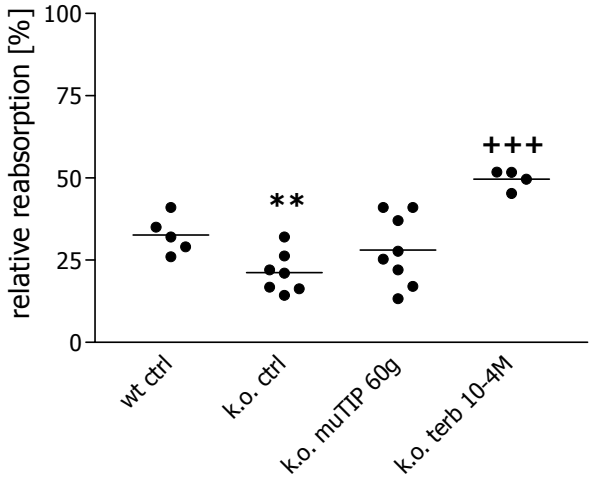

Figure 4.21: Relative liquid reabsorption in C57Bl/6 wt- and TNFR1/TNFR2 double-deficient- mice 60 min after instillation of 15 µl/g BW ringer lactate with 5% BSA containing muTIP(60µg), terbutaline (10^{-4}M). The lines represent the means of the individual values. ** $p<0.01$ for k.o. ctrl vs wt ctrl; +++ $p<0.0001$ for k.o. Terb vs k.o. ctrl. Unpaired t-test, two-tailed.

In summary, the function of the tip-peptide has been tested with different batches at various concentrations of the peptide in different mouse strains. Although there was a clear terbutaline-mediated increase of lung liquid clearance in all mouse strains, no significant effect could be detected upon tip treatment. Furthermore, an interfering signal caused by ventilation-induced TNF could be ruled out by using TNFR-deficient mice. Based on these observations there was no indication found for a tip-mediated effect in the flooded mouse lung model.

4.4.5 Role of the lectin-like domain within the TNF molecule in fluid-reabsorption

Despite of the above described observations concerning the tip-peptide, the lectin-like domain as a part of endogenous TNF has to be studied for an involvement in liquid reabsorption capacity of the cytokine. Since it has been shown in the previously described experiments that functionally relevant levels of TNF are produced in the lung upon experimental instillation and ventilation, the involvement of the lectin-like domain was investigated by comparing the basal liquid reabsorption between wt- and triple mutated k.i.- mice, the latter of which lack the lectin-like domain mediated activities.

Although the individual variations within the control animals (wt) were high, the performed experiments did not reveal a reduced lung liquid clearance in the k.i. mice, as compared to wt mice (Figure 4.22). This result does not indicate an impaired fluid reabsorption capacity in mice lacking the function of the lectin-like domain. Based on these observations, a role of the TNF tip-region in lung liquid clearance under physiological conditions appears to be unlikely.

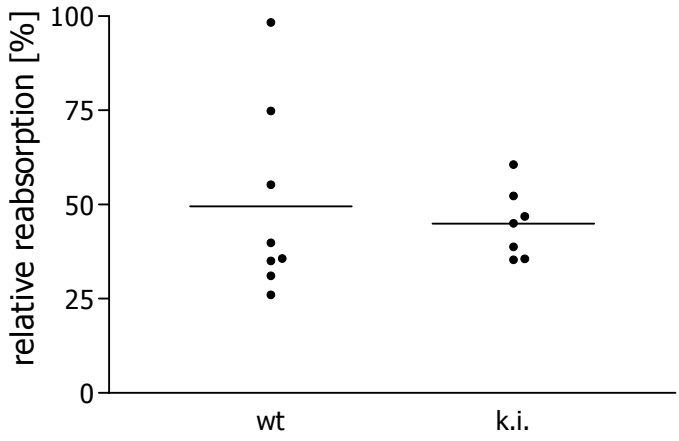

Figure 4.22: Relative liquid reabsorption in C57Bl/6 wt- and triple-mutated TNF k.i.- mice 60 min after the instillation of 15 µl/g BW ringer lactate with 5% BSA. The lines represent the means of the individual values.

4.4 The role of the lectin-like domain in the regulation of experimental *Trypanosoma brucei* infection

When investigating the role of TNF in a mouse model of African trypanosomiasis it has been previously demonstrated that the parasite peak levels of parasitemia were strongly increased in TNF k.o. mice, as compared to the peak levels recorded in wild-type mice. Furthermore, trypanosome-mediated immunopathological features, such as lymph node associated immunosuppression and lipopolysaccharide hypersensitivity, were found to be greatly reduced in infected TNF k.o. mice [153]. According to these and other investigations [53,134,152], TNF seems to be a key mediator involved in both parasitemia control and infection-associated pathology. Additionally, TNF was observed to directly kill the proliferating long slender bloodstream forms of *Trypanosoma brucei in vitro*, and the tip-region was identified as the trypanolytic domain of the cytokine [51]. In this context, the role of the lectin-like domain of TNF in the host-parasite interrelationship should be evaluated *in vivo* in experimental *Trypanosoma brucei* infections.

4.4.1 Analysis of TNF mediated lysis of T. brucei in vitro

The trypanolytic capacity of TNF was further investigated *in vitro* by treating bloodstream forms of *T. b. brucei* AnTat 1.1 with the mature (17 kDa) forms of (1) recombinant murine wt TNF, (2) recombinant murine triple-mutated TNF, (3) recombinant murine TNF lacking the receptor binding capacity, and (4) recombinant murine triple-mutated TNF lacking the receptor binding capacity.

These 17 kDa murine TNF proteins were obtained using the IMPACT^{TM}-CN system as described (4.1.2). Thereby, the functional properties of the murine wt TNF proteins either with or without mutated tip-region on different cell types have been reported above (chapter 4.1). Additionally, the TNF constructs without TNF receptor binding capacity have been proven to be unable to induce cytotoxicity on WEHI cells and on MF-R1-Fas/MF-R2-Fas cells, respectively (data not shown), implying that the inserted mutations (tyrosine^{86}→leucine) in fact led to a loss of the receptor binding capacity of the cytokine.

As shown in figure 4.24, a dose dependent lysis of the parasites was recorded for wt TNF and TNF without receptor binding capacity (R°). Significantly higher doses of R° TNF than of wt TNF were needed to kill the trypanosomes. In contrast, neither of the triple mutated TNF constructs, regardless of their receptor binding capacity, turned out to be trypanolytic. These results indicate that TNF does in fact directly kill the bloodstream form of *T. brucei in vitro*. Since a TNF mutant lacking the receptor binding capacity of the molecule is, while less effective, still able to induce trypanolysis, this effect seems to be receptor independent. Based on the total loss of the trypanolytic activity observed for triple-mutated TNF constructs, the conclusion can be drawn that the tip-region is the trypanolytic domain of the cytokine.

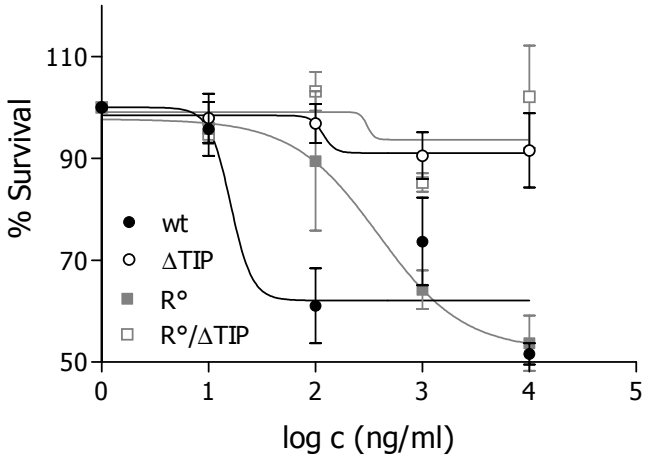

Figure 4.24: Survival of bloodstream forms of *T. brucei* in function of log concentration of (•) wt TNF; (°) TNF ΔTIP; (▪) TNF-R°; (▫)TNF-R°/ΔTIP. Trypanosomes were isolated from the blood of an infected mouse and incubated 4h in PSG (pH 8, +1% normal mouse serumg) at 37°C. n=3. Data are mean ± SEM.

4.4.2 Parasitemia development during T. brucei infection

In order to evaluate *in vivo* during experimental *Trypanosoma brucei* infections the role of the lectin-like domain of TNF in the host-parasite interrelationship, C57BL/6 wild-type as well as triple-mutated k.i. mice were infected by intraperitoneal injection of 5000 pleomorphic *T. brucei* AnTat 1.1 E parasites.

As shown in figure 4.25 the parasite proliferation in the blood of both infected mouse strains could be detected from day 35 of infection. Interestingly, whereas the parasite levels in wt mice remained comparatively low until death, triple-mutated k.i. mice exhibited significantly higher parasitemia counts. These findings point towards a role of the lectin-like domain of TNF in parasitemia control during experimental *T. brucei* infections.

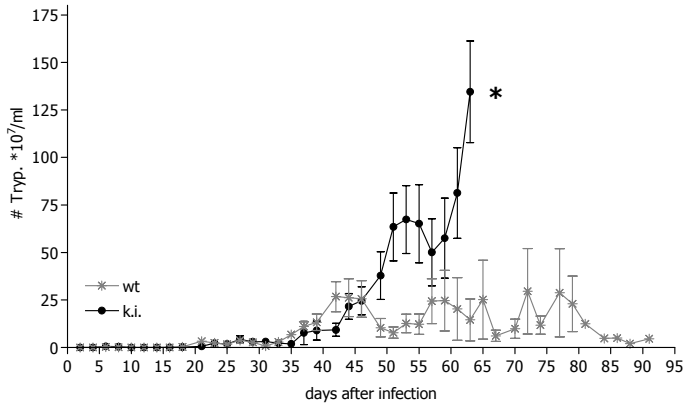

Figure 4.25: Parasitemia development of pleomorphic *T. brucei* AnTat 1.1 parasites in C57BL/6 wt (✳) and triple-mutated k.i. (•) mice. Nine male mice (all between 6 and 8 weeks of age) per group were infected at day 0 by intraperitoneal injection of 5000 parasites. Data are mean ± SEM. Unpaired t-test, two-tailed: $p<0.05$ for wt vs k.i..

4.4.3 Survival of T. brucei infected mice

Despite a significantly higher parasite load, the median survival times of *T. brucei* infected wt (62 days) and triple-mutated k.i. mice (56 days) were only slightly, but not significantly different (figure 4.26).

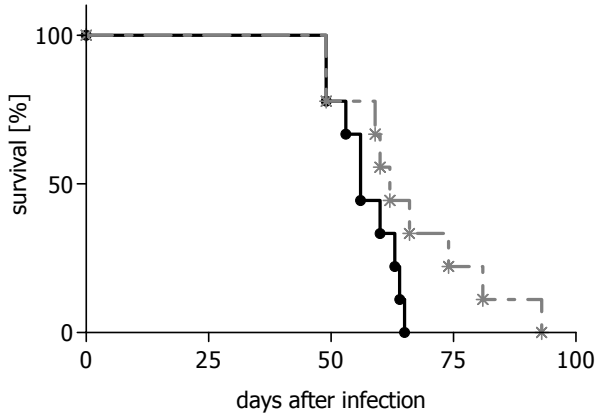

Figure 4.26: Survival of *T. brucei* AnTat 1.1 infected C57BL/6 wt (✳) and triple-mutated k.i. (•) mice. Nine male mice (all between 6 and 8 weeks of age) per group were infected at day 0 by intraperitoneal injection of 5 000 parasites.

4.4.4 Cachexia development in T. brucei infected mice

Up to day 56 (median survival time of infected k.i. animals) of infection, when at least half of the animals in each experimental group are still alive, the cachexia observed in k.i. mice was increased with high significance, as compared to wt mice ($p=0.0001$; two tailed t-test). Thus, infection-associated weight loss was more pronounced in triple-mutated k.i. mice than in infected wt mice (Figure 4.27).

The trypanosomal infection-associated cachexia is a pathological finding that has been reported to be mediated by TNF [180]. Since the weight loss detected in the current model was even increased in the triple-mutant k.i. mice the lectin-like domain of TNF seems to be either directly or indirectly implicated in the regulation of infection-associated pathology.

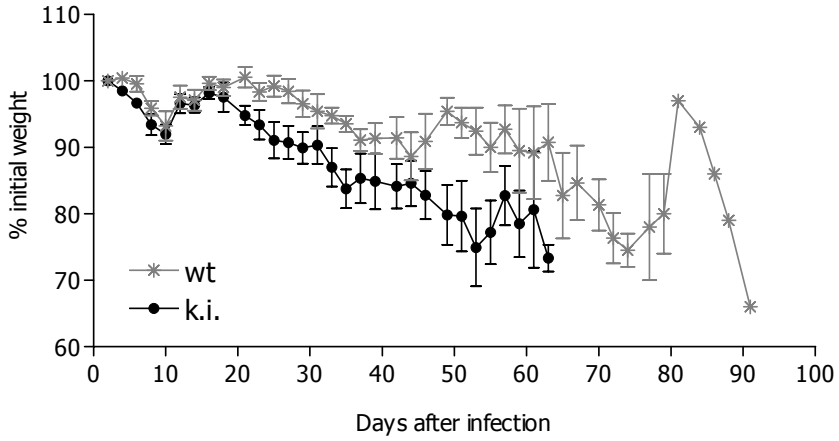

Figure 4.27: Alterations in individual body weight of *T. brucei* AnTat 1.1 infected C57BL/6 wt (✳) and triple-mutated k.i. (•) mice. Nine male mice (all between 6 and 8 weeks of age) per group were infected at day 0 by intraperitoneal injection of 5,000 parasites. Data are mean ± SEM.

4.4.5 Role of the interaction between triple-mutated TNF and TNFR2 in the regulation of experimental T. brucei infection

The recently published analysis of *T. brucei* infections in 4 different established, conventional mouse models, as well as in TNF-deficient and TNF-receptor-deficient mice indicated the following: (1) during experimental *T. brucei* infections, TNFR2 signaling plays a key role in the induction of pathology; and (2) the increased ratio of TNF over its soluble receptor 2, not TNF per se, relates to the occurrence of infection-associated pathology, such as weight loss [158]. In this context it is important that the triple-mutant of TNF displays a significantly reduced TNFR2 mediated bioactivity *in vitro* as compared to wt TNF. Accordingly, the increased weight loss observed in the infected triple-mutated k.i. mice could be based on altered interactions between triple-mutated TNF and TNFR2. To address this question, an additional experimental series was carried out, in which TNFR2 deficient mice as well as triple-mutated k.i. and wild type mice were infected.

4.4.6 Parasitemia development during T. brucei infection

As reported in figure 4.28, a low initial parasitemia peak with up to 2.10^8 parasites/ml in wt and k.i. mice and up to 5.10^8 parasites/ml in TNFR2 k.o. mice occurred around day 15 of infection. This initial peak was followed in wt and triple-mutated k.i. mice by a sustained parasitemia, during which parasites were hardly detectable in the blood circulation until day 40 of infection. Starting from day 50 the parasites proliferated faster in triple-mutated k.i. mice than in wt mice, unlike in TNFR2 deficient mice where the parasite burden was raised only 3 days after the clearance of the initial peak, namely at day 20.

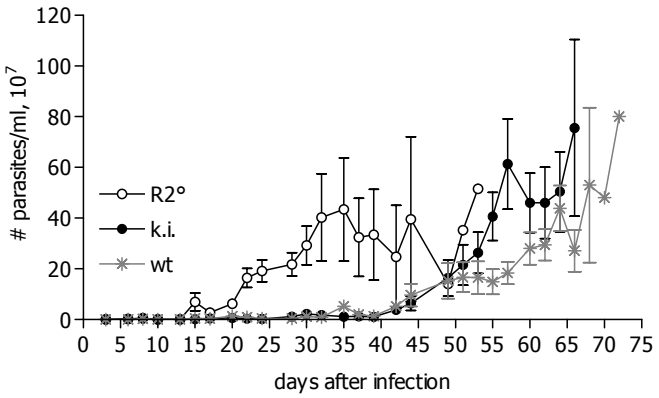

Figure 4.28: Parasitemia development of pleomorphic *T. brucei* AnTat 1.1 parasites in C57BL/6 wt (✳), triple-mutated k.i. (•), and TNFR-2 deficient (°) mice. Eight female mice (all between 6 and 8 weeks of age) per group were infected at day 0 by intraperitoneal injection of 5 000 parasites. Data are mean ± SEM

4.4.7 Survival of T. brucei infected mice

When scoring survival rates (Figure 4.29), statistically significant differences in survival were recorded in the TNFR2-deficient animals, as compared to the other groups of infected mice. However, the difference between triple-mutated k.i. mice and wt mice was marginal and statistically not significant.

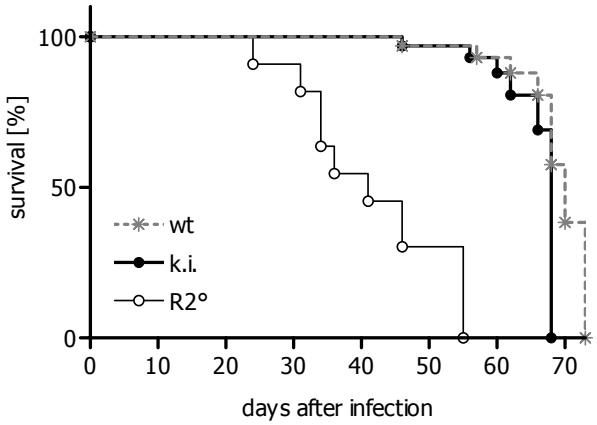

Figure 4.29: Survival of *T. brucei* AnTat 1.1 infected C57BL/6 wt (*), triple-mutated k.i. (•), and TNFR-2 deficient (°) mice. Eight female mice (all between 6 and 8 weeks of age) per group were infected at day 0 by intraperitoneal injection of 5000 parasites.

4.4.8 Cachexia development in T. brucei infected mice

Despite the similar survival times, the cachexia observed in k.i. mice was again significantly ($p<0.05$, unpaired t-test) increased, as compared to wt mice. According to the results presented in figure 4.30, the k.i. animals lost about 25% of their initial weight until death, whereas the weight of infected wt mice was nearly unaltered. In TNFR2-deficient mice infection-associated weight loss was even more pronounced. Whereas these mice gained 12% weight during the early state of infection, they showed an overall weight loss of about 40% from day 30 on. These findings suggest that both the lectin-like domain of TNF and TNFR-2 play a crucial role in infection-associated cachexia.

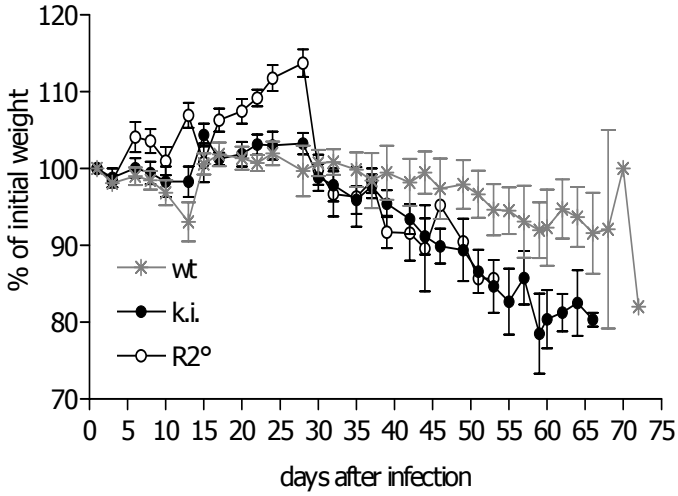

Figure 4.30: Alterations in individual body weight of *T. brucei* AnTat 1.1 infected C57BL/6 wt (*), triple-mutated k.i. (•), and TNFR-2 deficient (°) mice. Eight female mice (all between 6 and 8 weeks of age) per group were infected at day 0 by intraperitoneal injection of 5 000 parasites. Data are mean ± SEM.

4.4.9 Circulating serum TNF levels during T. brucei infections

Because TNF was reported to play a crucial role in the capacity of mice to control parasite levels, as well as their trypanosomiasis-associated pathology [153], circulating TNF levels have been analyzed. Since the amounts of serum gained from the infected animals were restricted, the probes had to be pooled for this TNF measurement. As such, variations between individual animals could not be detected. Nevertheless, according to the results indicated in figure 4.31, TNF was detectable in each of the infected mouse strains. The TNF level at day 22 of infection was similar in triple-mutated k.i. and TNFR2-deficient mice, whereas equal amounts of TNF in sera of wt and triple-mutated k.i. mice could be detected at day 31. Furthermore, TNF serum levels in wt and TNFR2-deficient mice turned out to be similar at day 38 of infection. Based on these observations it can be concluded that, despite of the variations between different time points, the cytokine levels appeared to be comparative in all strains.

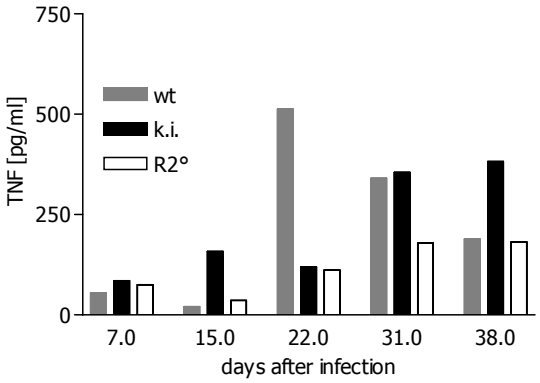

Figure 4.31: TNF serum levels in *T. brucei* AnTat 1.1 infected C57BL/6 wt, triple-mutated k.i. ,and TNFR-2 deficient mice. Eight female mice (all between 6 and 8 weeks of age) per group were infected at day 0 by intraperitoneal injection of 5 000 parasites. The probes were pooled and ¼ diluted for TNF measurement.

4.4.10 Anti-trypanosome immunoglobulin induction during T. brucei infections

The immune defence against parasites normally involves the generation of a specific antibody population. Also for trypanosomal infections an elevated level of antibodies directed against the surface antigen (VSG) has been described [181]. Whether TNF is involved in the initiation of antibody production is not clear so far. Therefore, the progressive course of antibody concentration in the serum of infected mice was analysed by ELISA. The results shown in figure 4.32 indicate that wt mice, triple-mutated k.i. mice, and TNFR2-deficient mice produced similar humoral antitrypanosome responses during an experimental *T. brucei* infection. In all infected mouse strains, the levels of IgM and IgG anti-trypanosome antibodies increased significantly between day 21 and day 28 of infection. At this time, the parasitemia levels in TNFR2-deficient mice were already high, whereas the parasite proliferation in the blood of infected wt and triple-mutated k.i. mice could be detected not before day 40 of infection. According to these observations it can be concluded that the specific immune response is not affected by a modified TNFR2 signaling. Furthermore, the antibody response seems not primarily determine the prevention of parasite growth during experimental trypanosomiasis in mice.

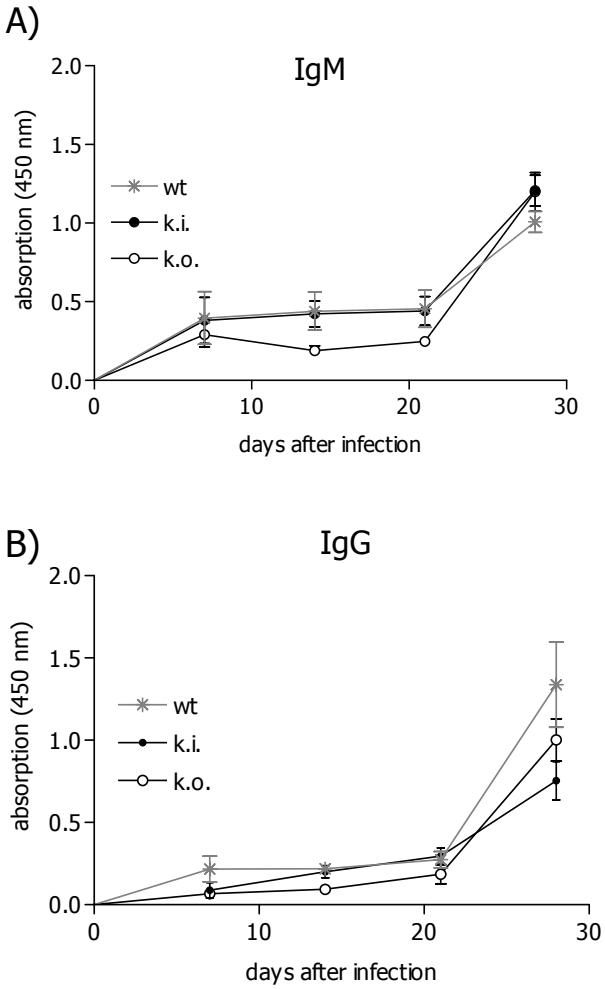

Figure 4.32: Development of an antiflagellar pocket immune response during experimental infection with *T. brucei* AnTat 1.1. Antibody levels were measured in the serum of infected wt, triple-mutated k.i., and TNFR2-deficient mice. Background absorption caused by aspecific binding was determined by employing preimmune serum and substracted from the absorption of the samples. For antibody measurement the probes were diluted 1/80. n=4; data are mean ± SEM.

In summary, the findings suggest that both the lectin-like domain of TNF and TNFR2 play a crucial role in parasitemia control and infection-associated cachexia, whereas the specific anti-VSG antibodies do not seem to be involved. As shown previously, the triple-mutant of TNF has a reduced TNFR2 mediated bioactivity as compared to wt TNF. Accordingly, the increased cachexia observed in triple-mutated k.i. mice, as compared to wt mice, could be attributed to altered interactions between triple-mutated TNF and TNFR2.

5. Discussion

5.1 A triple-mutant TNF k.i. mouse as a tool for investigating the role of the lectin-like domain of TNF *in vivo* under normal and pathological conditions

In the present study the role of the lectin-like domain of TNF in alveolar liquid clearance and during experimental African trypanosomiasis was investigated *in vivo*. To that purpose a triple-mutant TNF knock-in mouse, expressing TNF that lacks the trypanolytic activity of the cytokine was generated. As a result of the identification of several offspring genotypes, the mutation was passed to the outcome according to the prediction of Mendel`s law, implying that the inserted mutations are not lethal. Because TNF-deficient mice were described to be viable and fertile [182], the normal development of the k.i. animals, lacking the function of just a single domain of TNF, was not surprising.

Upon treatment with LPS *in vivo*, the k.i. mice were able to produce physiologically relevant amounts of TNF. Furthermore, LPS treatment of peritoneal macrophages isolated from k.i. mice and wt mice, respectively, resulted in comparable levels of TNF secretion. The investigation of ventilation-induced TNF secretion in the lungs revealed similar TNF levels in the alveolar fluid of both mouse strains.

In summary, nucleotide substitutions in the TNF coding sequence do not cause drastic changes concerning the secretion of the protein. Therefore, the triple-mutated TNF k.i. mouse is an appropriate tool to investigate the role of the lectin-like domain of TNF *in vivo*, under normal and pathological conditions.

5.2 Role of the lectin-like domain of TNF *in vivo* in alveolar liquid clearance

The reabsorption of alveolar fluid in acute bacterial pneumonia in rats has been reported to be upregulated by a TNF-dependent mechanism [183]. A more recent article confirmed that TNF could augment alveolar epithelial fluid transport in a model of septic peritonitis in rats [184]. Moreover, the instillation of exogenous TNF into the lungs of anaesthetized and ventilated rats resulted in an upregulated lung liquid clearance, whereas a triple-mutant TNF, lacking the lectin-like activity of the cytokine showed no effect [166]. Therefore, the promoting effect of TNF on edema reabsorption seems to be linked to its lectin-like domain. Thus, recent studies revealed that instillation of a peptide mimicking the lectin-like domain of TNF, the so-called tip-peptide, was able to increase the clearance of liquid from the lung as well [58,129]. However, the role of the lectin-like domain as a part of endogenous TNF has not been explored so far.

To determine the function of the TNF tip-region *in vivo* under physiological conditions, a triple mutant TNF k.i. mouse was generated in the work presented here. Furthermore, a suitable mouse model with intact epithelial and endothelial barriers, the *in vivo* flooded mouse lung model, was established to study lung liquid clearance in intact anaesthetized and ventilated mice.

For the human tip-peptide an induction of fluid reabsorption has been reported in rats [129]. In the study presented here, the knowledge about the reabsorption capacity in mice has been extended. The flooded mouse lung model is a quite invasive method that includes anaesthesia and tracheotomy. To obtain reliable results it was very important to evaluate the basic experimental conditions regarding a stress-induced β-adrenergic stimulation.

Since a lot of studies proved the capacity of β_2-agonists to stimulate fluid clearance[89,90,97,185-187], the influence of the potent β_2-antagonist propranolol was investigated. Despite of high drug dosage the lung liquid reabsorption was not significantly reduced under the applied conditions. Moreover, inhibition of the active sodium transport across the epithelial barrier by amiloride completely inhibited the fluid efflux from the alveolar space (data not shown). On the one hand, these experiments indicate that the experimental conditions do not provoke an increased

fluid reabsorption due to β-adrenergic stimulation. On the other hand, the inhibition capacity of amiloride proves the integrity of the lung epithelium in the mouse model. Whereas the inhibition of β_2-receptors had no effect on basal fluid reabsorption, treatment with the β-adrenergic agonist terbutaline resulted as expected in the induction of water reabsorption. This effect clearly proves that the *in vivo* flooded mouse lung model is an appropriate tool to detect the effect of substances on fluid reabsorption capacity in mice.

In sharp contrast to terbutaline, treatment with the tip-peptide failed to induce an increase in alveolar fluid reabsorption in mice. This observation was independent of the species specific sequence of the peptide (murine, human) and the mouse strain treated (Balb/c, C57Bl/6). Furthermore, increasing the dosage did not lead to a significant effect on fluid reabsorption as well. Based on these findings, there is no evidence for an effect on lung liquid clearance in the flooded mouse lung model.

As mentioned before, TNF exerts both a positive and a negative effect on the regulation of intrapulmonary liquid [112-116]. It is relevant in this context that high tidal volume ventilation per se (34.5 ml/kg BW), without any preceding lung injury, has been reported to induce intrapulmonary TNF upregulation in mice [179]. Assuming a mouse weight of 25 g, the published high tidal volume of 34.5 ml/kg corresponds to a tidal volume of 800 µl. In the mouse model presented in this work, mice were ventilated with a volume of 200 µl and 400 µl of liquid were additionally instilled into the distal airspaces. The summed volume of 600 µl could result in the induction of intrapulmonary TNF expression. In fact, TNF was detected in both mouse strains, indicating a secretion of this cytokine caused by the experimental conditions. These observations raised the question whether the amount of basally produced TNF was able to affect lung-liquid clearance via a TNF receptor-dependent mechanism, interfering with the clearance effect primarily induced by treatment with exogenous tip-peptide. To this purpose, the basal level of edema reabsorption after 60 min of ventilation was determined in TNFR1/TNFR2 double deficient mice. Strikingly, the basal edema reabsorption capacity was decreased in these mice as compared to wt mice. This finding points towards a TNFR-dependent promoting effect of basally produced endogenous TNF on lung liquid clearance in the current model. In the literature, the receptor-mediated effects of TNF are predominantly discussed to lead to increased vascular permeability and edema formation [188], whereas the promoting

effect of the cytokine on the reabsorption of intrapulmonary liquid, mediated by its lectin-like domain, have been reported to be receptor independent [58]. Because the triple-mutant TNF completely lacked the ability to promote lung liquid clearance in rats, this assumption seems to be plausible. But this interpretation could be incomplete, since the triple-mutant TNF showed a significantly reduced TNFR2-mediated bioactivity *in vitro* and even a reduced affinity for TNFR1 (5-fold) and TNFR2 (10-fold) [54]. Therefore, the functional lack of the mutated TNF could also be due to altered interactions with the receptors. Indeed, antibodies directed against TNFR1 and TNFR2 efficiently blocked the sodium uptake-activating effect of TNF on A549 cells [166], implying that this effect is dependent of TNFR1, TNFR2 or both. On the other hand, the edema reabsorption promoting effect of TNF in a flooded mouse model *in situ* was equal in TNFR1 and TNFR2 deficient mice, respectively [58].

However, the mechanism by which TNF increases the reabsorption of intrapulmonary liquid *in vivo* may be considerably more complicated and may involve multiple pathways. Via its receptors, TNF might stimulate the release of other mediators, such as transforming growth factor-α [112,116] which has been shown to rapidly upregulate alveolar liquid clearance in rats [189].

The tip-peptide was described to act independently of either TNFR [51]. By using TNFR1/TNFR2 double deficient mice the promoting effect of the basally produced endogenous TNF in the *in vivo* flooded mouse lung model was eliminated. Even under these experimental conditions, no significant increase on fluid reabsorption could be detected. Therefore, a TNF receptor-independent action of the peptide that interferes with receptor-dependent actions of endogenous TNF is clearly excluded. Accordingly, there was no indication for a tip-mediated effect in the flooded mouse lung model.

Although there is no experimental evidence for a tip-peptide mediated effect, the lectin-like domain as a part of endogenous TNF could be involved in liquid reabsorption capacity of the cytokine. Since functionally relevant levels of TNF are produced in the mouse lung upon experimental instillation and ventilation, the role of the lectin-like domain was investigated by comparing the basal liquid reabsorption in wt and triple mutated k.i. mice, with the latter lacking the lectin-like domain mediated effects. Since concentrations of endogenous TNF in the residual lung liquid of both mouse strains were on the same level, a selective influence of the basally

produced TNF on one experimental group is excluded. As a result, no impaired fluid reabsorption capacity in mice lacking the function of the lectin-like domain could be detected. Based on these observations, a role of the TNF tip-region on lung liquid clearance under physiological conditions appears to be unlikely in the model tested.

In summary, no significant effect on edema reabsorption could be detected upon tip-treatment, although there was a clear terbutaline-mediated increase on lung liquid clearance in the applied *in vivo* flooded mouse lung model. This observation was independent of the mouse strain and of the dose and the species of the appropriate tip-peptide. Furthermore, an interfering signal caused by ventilation-induced intrapulmonary TNF secretion could be ruled out. In addition to the observations concerning the tip-peptide, there was no indication for a role of the lectin-like domain as a part of endogenous TNF in the regulation of intrapulmonary liquid reabsorption *in vivo* in the models investigated.

5.3 Experimental African trypanosomiasis in mice: Role of the lectin-like domain in the control of parasitemia and infection-associated pathology

The accumulated knowledge about the trypanosome-elicited production of TNF indicates that this cytokine exerts dual effects during trypanosome infections, influencing both the parasite and the host. As such, the induction of TNF production during trypanosome infections could be either beneficial or devastating for the host. Thus, it has been shown that TNF-deficient mice exhibited upon *Trypanosoma brucei* infection significantly increased parasitemia but showed at the same time strongly reduced infection-associated pathology [153]. These results point towards a double-edged role of TNF during trypanosome infections in both parasitemia control and infection-associated morbidity. On the one hand the role of TNF in trypanosomosis-associated immunopathology has been suggested in several studies, showing (1) an enhanced expression of TNF in the brains of *Trypanosoma brucei* infected mice [190], (2) the association between TNF production by monocytes and the severity of disease-associated anemia in *Trypanosoma*-infected cattle [156], (3) the correlation between serum TNF levels and neuropathological symptoms in human sleeping sickness patients [148], and (4) the involvement of TNF in trypanosome-elicited immunosuppression and overall morbidity [52,191]. On the other hand, the role of TNF in parasite control could be due to the ability of the cytokine to directly kill the proliferating long slender bloodstream forms of *Trypanosoma brucei* that has been observed *in vitro*. Because a triple-mutated TNF, lacking the lectin-like activity of the cytokine, has not been trypanolytic at all, the trypanolytic activity of TNF seems to be linked to its lectin-like domain. Accordingly, the tip-region was already identified as the trypanolytic domain of TNF in a previous study [51]. Furthermore, a TNF mutant lacking the receptor binding capacity of the molecule was, while less effective, still able to induce trypanolysis, implying that this effect seems to be receptor-independent.

In the present study, the role of the lectin-like domain of TNF in the host-parasite interrelationship has been evaluated *in vivo* during experimental *Trypanosoma brucei* infections. To this purpose, triple-mutated muTNF k.i. mice, expressing TNF that lacks the lectin-like activity of the cytokine, have been infected. As observed in TNF-

deficient mice [153], triple-mutated muTNF k.i. mice showed an increased parasite load, as compared to wild-type mice. The equivalent results from infected TNF-deficient [153] and triple-mutated k.i. mice indicate that the lectin-like domain of TNF is implicated in TNF-mediated control of parasitemia.

The weight-loss (cachexia) associated with trypanosomal infection is a pathological finding that has been reported to be mediated by TNF [180,192]. Since cachexia was more pronounced in infected k.i. than in wt mice, the lectin-like domain might even participate in the control of infection-associated pathology. Thus, the lack of the lectin-like activity during trypanosomal infection appears detrimental for the morbidity of the host, while the complete absence of TNF was, as mentioned before, even beneficial. Due to the similar development of parasitemia and the differences in infection-associated pathology in TNF-deficient and triple-mutated k.i. mice, respectively, pathology is obviously not correlated with parasite levels. This conclusion corresponds to previously obtained results of a comparative analysis of 4 *T. brucei* mouse models, including two models for high infection-associated pathology (CeH/HeN and C57Bl/6) and two models for low infection-associated pathology (BALB/c and CBA/Ca). This study also did not reveal a correlation between peak parasitemia control and loss of body weight [158].

Although TNF was shown to mediate some of its harmful effects by inducing cachexia, circulating TNF serum levels were not correlated with infection associated weight loss in mice [158]. Furthermore, two recent independent studies, performed on a large-scale sampling of patients with human sleeping sickness, found no correlation between pathology and TNF serum levels [133,157].

The extracellular domains of both TNF receptors can be released into the circulation by proteolytic cleavage [43]. The resulting soluble molecules are able to neutralize biological activities of TNF [47]. Accordingly, plasma from acutely *T. cruzi* infected mice has the capacity to neutralize TNF, since it is able to significantly inhibit the TNF-mediated cytotoxic activity on WEHI cells. Such neutralizing activity is correlated with soluble TNFR2 levels but not with levels of soluble TNFR1 [192]. These observations strongly argue for the involvement of soluble TNFR2 in the neutralizing activity found in plasma from infected mice. Also, soluble TNFR2 has been reported to play a key role in the protection from pathology during experimental *T. brucei* infection. Moreover, the increased ratio of TNF over its soluble receptor 2, rather than TNF per

se, correlated with the occurrence of infection-associated pathology, such as weight loss [158]. In this context it is interesting to note that a significantly reduced TNFR2-mediated bioactivity of triple-mutant TNF as compared to wt TNF has been shown in this work. Accordingly, the increased weight loss observed in the infected triple-mutated k.i. mice could be based on a reduced affinity of triple-mutated TNF to bind TNFR2. Such a reduced binding affinity might result in a decreased capacity of soluble TNFR2 to neutralize TNF in the serum of infected mice, subsequently leading to a stronger inflammatory response of the cytokine. Indeed, in TNFR2-deficient mice completely lacking the TNF neutralizing ability via soluble TNFR2, an infection-associated weight-loss was observed. This observation strongly supports the hypothesis that the cachexia found in triple-mutated k.i. mice was at least in part provoked by a decreased capacity of TNFR2 to neutralize the mutated TNF.

When scoring for survival rates, statistically significant differences in survival were recorded in the TNFR2-deficient animals, as compared to k.i. and wt animals. However, the median survival time of infected k.i. mice was slightly reduced. Since TNF mutation impairs but does not abolish interaction with TNFR2, the difference between TNFR2 deficient mice and triple mutated k.i. mice is not surprising.

In patients with human sleeping sickness, infection-associated mortality results from parasite infiltration through the blood-brain barrier [193]. Although it is unclear how parasites are able to cross the endothelial blood brain barrier at certain infection stages, this may be caused by a change in endothelial cell properties due to a persistent inflammatory environment [194]. Therefore, the significantly shortened survival of TNFR2-deficient, and even the slightly reduced survival times of triple-mutated k.i. mice might be a consequence of missing or reduced TNF neutralization by soluble TNFR2. Consequently, this altered neutralization process could cause an accelerated inflammation-induced damage of the endothelial blood brain barrier, enabling the parasites to infiltrate the brain earlier during infection.

TNFR2-deficient mice did not show a decreased parasite burden as compared to wt mice. In contrast, the parasites were detected earlier in the circulation and an enhanced proliferation was found. Discussing a neutralizing effect of TNFR2 on TNF in experimental trypanosomiasis, this observation is rather surprising. Given the fact that the TNFR2-deficient mice lacked neutralization by the soluble TNFR2, there should be a TNF overcapacity, mediating for example the lysis of the parasites.

Hence, the trypanolytic activity of TNF that was found *in vitro* does not seem to play an ascertainable role in this context. Rather, the involvement of TNF in the pathway of immunosuppression caused by *T. brucei* [195] could be a reason for the relatively high parasitemia levels recorded in TNFR2-deficient mice. Moreover, it also seems likely that indirect host responses are involved in parasite control and occurrence of pathology.

In conclusion, the data presented in this work suggest that the lectin-like domain of TNF most likely via TNFR2 plays a crucial role in parasitemia control and infection-associated cachexia. Since the triple-mutant of TNF was shown to have a reduced TNFR2-mediated bioactivity as compared to wt TNF, the increased cachexia observed in triple-mutated k.i. mice could be attributed to reduced interactions between TNF and soluble TNFR2.

5.4 The role of the lectin-like domain of TNF in receptor activation

TNF occurs as a type II membrane protein and a soluble form resulting from proteolytic processing of the membrane bound precursor [42]. These two forms of the cytokine were shown to mediate different bioactivities via TNFR2 but there are no variances with respect to TNFR1 signaling [31].

Apart from the interaction with its two receptors, TNF also has a lectin binding capacity for specific oligosaccharides, such as chitobiose and branched trimannoses[49]. This lectin-like domain of TNF was previously identified and found to be located in the tip-region when looking at the three-dimensional structure of the TNF trimer. The lectin-like region has been reported to be both functionally and spatially separated from the protein-protein interaction sites with the receptors [51]. However, there are hints from the literature for a role of the lectin-like domain in the signal transduction of soluble TNF via TNFR2 [54], although the previously used systems did not clearly distinguish between the two receptor forms. Moreover, TNFR2 can only be efficiently activated by transmembrane TNF, in contrast to TNFR1 which is activated to the same extend by both forms of the cytokine [31]. Based on these features the role of the lectin-like domain in TNFR1/TNFR2 activation of soluble and transmembrane TNF has been further investigated in this study. To this purpose, a recombinant lectin-deficient triple mutant of mature TNF, in which the three amino acids critical for its lectin-like activity were replaced by alanines, was generated. This triple-mutant of murine TNF showed a 5-fold reduced capacity to induce cytotoxicity in WEHI cells as compared to wt TNF. In contrast, the mutated TNF protein turned out to be slightly more potent in HepG2 cells than wt TNF. Since HepG2 cells exclusively express TNFR1 [164] these observations indicate that the inserted mutations do not impair the TNFR1 activation. Provided that cytotoxicity in WEHI cells is mediated by both receptors, the reduced capacity of the triple mutant has to be attributed to a decrease in TNFR2 signalling.

To further prove the functional consequence of the tip mutation with respect to TNFR1 and TNFR2 dependent mechanisms, immortalized murine fibroblasts stably expressing receptor chimeras were used. These engineered receptor variants were derived from the extracellular domains of the two human TNF receptors and the intracellular death domain of human Fas (MF-R1-Fas; MF-R2-Fas). In a recent study

Krippner-Heidenreich et al demonstrated that the chimeric R1-Fas/ R2-Fas receptors as well as the wild type TNF receptors exhibit identical activation requirements regarding the soluble and membrane-bound TNF [161]. As demonstrated in HepG2 cells, the cytotoxic capacity of soluble wt TNF and triple-mutated TNF in MF-R1-Fas cells was nearly the same. This finding strengthens the prediction that the inserted mutations do not influence TNFR1-mediated activity, implying that the tip-region is not involved in soluble TNF/TNFR1 induced signal transduction. In correlation with the published finding that TNFR2 can only be efficiently activated by transmembrane TNF [31], only a slight cytotoxic effect could be observed on MF-R2-Fas cells when treated with soluble TNF.

To observe the role of the lectin-like domain of TNF in transmembrane TNF-mediated TNFR2 activation, an available tool that mimics transmembrane signalling has been used in this study. The TNFR2-specific monoclonal antibody 80M2 combined with soluble TNF induces intracellular signals comparable with the transembrane form of TNF has been recently described [31]. Treatment of MF-R2-Fas cells with the recombinant TNF proteins in combination with 80M2 revealed that the cytotoxicity induced by the triple mutated TNF was significantly reduced as compared to wt TNF. Therefore, the lectin-like domain is involved in the signal transduction of both transmembrane and solube TNF via TNFR2.

It has been shown in a recent study that the triple-mutant had a 5-fold lower relative affinity for the soluble TNFR1 and a 10-fold-lower relative affinity for the soluble TNFR2 than wt TNF [54]. However, the data presented here demonstrate that the reduced affinity supposed is not reflected in a decreased signal intensity for the TNFR1 on a living cell. Otherwise, the observed about 10-fold lower relative affinity correlates with the findings of a reduced capacity in cell death induction for the TNFR2.

Mutant TNF may show reduced cytotoxicity for several reasons: the subunit may not fold correctly, the trimer may not form correctly, or interaction with the receptor may be altered. To check whether the reduced TNFR2 activation of triple-mutated TNF was due to an impaired trimer formation, the TNF preparations where treated with the chemical cross-linker EGS. As a result no differences in multimere formation could be observed, indicating that the mutations in the tip-region do not affect the

physiological formation of TNF trimers. Consequently, the reduced capacity could be attributed to an obstruction of direct contact of the tip region with the TNFR2.

In summary, the lectin-like domain of TNF was shown to be involved in the activation of TNFR2 by both soluble TNF and transmembrane TNF. However, a role of this TNF region in TNFR1 mediated signal transduction could be ruled out, since the induction of TNFR1 by the triple-mutant of TNF, lacking the lectin-like activity of the cytokine, was similar to that of wt TNF.

6. Summary

Apart from the interaction with its two receptors, TNF also exhibits a lectin binding capacity for specific oligosaccharides. Although the lectin-like region has been reported to be functionally and spacially separate from the interaction sites with the receptors a role of this TNF domain in the signal transduction of soluble TNF via TNFR2 was suggested. Therefore, using mouse fibroblasts stably expressing receptor chimeras derived from the extracellular domain of the two human TNF receptors and the intracellular death domain of human Fas (MF-R1-Fas/MF-R2-Fas), the involvement of the lectin-like domain in TNFR1/TNFR2 activation of soluble and transmembrane TNF was further investigated. Hence, the lectin-like domain of TNF was shown to be involved in the activation of TNFR2 by both soluble TNF and transmembrane TNF. However, a role of this TNF region in TNFR1 mediated signal transduction could be ruled out, since the induction of TNFR1 by the triple-mutant of TNF, lacking the lectin-like activity of the cytokine, was similar to that of wt TNF.

The capacity of TNF to promote lung edema reabsorption and the ability to directly kill the bloodstream forms of *African trypanosomes in vitro* has been linked to the lectin-like domain of the cytokine. Thus, a peptide mimicking this TNF region, the so-called tip-peptide, exerts both activities as well. To further investigate the function of the lectin-like domain *in vivo* under physiological and pathological conditions, triple-mutated TNF knock-in-mice (B6-TNF$^{TM1.1Blt}$), expressing TNF that lacks the trypanolytic activity of the cytokine, have been generated. These mice are viable and fertile. Moreover, the processing of the cytokine is not drastically changed.

An *in vivo* flooded mouse lung model was established to observe the role of the lectin-like domain in lung liquid clearance. Hence, there was no indication for a role of this TNF domain in the regulation of intrapulmonary liquid reabsorption. Moreover, although for human tip-peptide an induction of lung liquid clearance has been reported in rats, no significant effect on edema reabsorption could be detected in the mouse model. This observation was independent of the mouse strain and of the dose and the species specific sequence of the peptide (human, murine).

However, the lectin-like domain participates in the host-parasite interrelationship during experimental *Trypanosoma brucei* infections *in vivo*. Infection of triple-mutant k.i. mice resulted in increased parasitemia levels and infection associated pathology,

when compared to wt mice. In TNFR2-deficient mice, lacking a soluble TNFR2 mediated neutralization of TNF, these effects were even more pronounced. Accordingly, it is concluded that the trypanolytic activity of TNF that was found *in vitro* does not seem to play an ascertainable role in this context. Rather the involvement of TNF in the pathway of immunosuppression caused by *T. brucei* or indirect host responses could be a reason for the relatively high parasitemia recorded in TNFR2 deficient mice. Keeping in mind that the triple-mutant of TNF displayed a reduced TNFR2-mediated bioactivity as compared to wt TNF, the increased cachexia observed in triple-mutated k.i. mice could be attributed to reduced interactions between TNF and the neutralizing soluble TNFR2.

7. Zusammenfassung

Neben seiner Eigenschaft an die TNF-Rezeptoren zu binden, besitzt das TNF-Molekül eine lektin-artige Affinität für Chitobiose und Trimannosen. Diese Bindungsstelle ist räumlich von der Rezeptorbindungsdomäne getrennt und wird als Tip-Domäne bezeichnet. Für die Funktion der lektinartigen Domäne sind drei Aminosäuren essentiell. Zur Analyse der Tip-Region wurden durch den Austausch dieser Aminosäuren loss of Mutanten generiert.

Es gibt Hinweise für eine Beteiligung der Tip-Domäne bei der Aktivierung des TNFR2. Aus diesem Grund wurde die Funktion dieses TNF Abschnitts in der vorliegenden Arbeit näher untersucht. Da die biologische Wirkung der Signaltransduktion des nativen TNFR2 nur schwer erfassbar ist, wurden Zellinien verwendet, die die extrazelluläre TNFR-Domäne und einen intrazellulären Teil des Fas-Rezeptors stabil exprimieren. Anhand dieser Rezeptorchimeren konnte belegt werden, daß für eine effektive Induktion des TNFR2 eine intakte Tip-Domäne essentiell ist. Die Mutation dieses TNF-Bereiches hat bezogen auf die Aktivierung des TNFR1 dagegen keine Konsequenz.

Durch bisher wenig geklärte Mechanismen fördert TNF über seine Tip-Domäne die Resolution von Lungenödemen und induziert *in vitro* die Lyse von afrikanischen Trypanosomen. Für die genauere Untersuchung der Funktion des Tip-Gebietes *in vivo* wurden im Rahmen dieser Arbeit dreifach-mutierte k.i. Mäuse generiert (B6-TNF$^{TM1.1Blt}$). Es zeigte sich, daß der mutationsbedingte Funktionsverlust der lektinartigen Domäne keinen Einfluß auf die Vitalität und Fertilität der Tiere hat. In dem im Rahmen dieser Arbeit etablierten *in vivo* flooded Lung-Modell wurde kein Hinweis für eine Beteiligung der Tip-Domäne an der Flüssigkeitsresorption aus der Lung erhalten. Da auch synthetische Tip-Peptide unabhängig von ihrer speziesspezifischen Sequenz (Mensch, Maus) und den verwendeten Mausstämmen (C57Bl/6, BALB/c) keinen signifikanten Effekt zeigten, kann die Funktion der Tip-sequenz bei der Ödemresorption in der Maus nicht bestätigt werden.

Im Gegensatz zur Ödemresorption zeigen die aus den Versuchen zur experimentellen Trypanosomiasis erhobenen Daten eine Rolle der Lektin-Domäne bei der gegenseitigen Wechselwirkung zwischen Wirt und Parasit an. Infizierte k.i. Mäuse wiesen im Vergleich zu wt Mäusen eine erhöhte Parasitämie und eine ausgeprägte

Pathologie auf. Da diese Symptome ebenfalls bei TNFR2 k.o. Mäusen auftraten, wird hier einerseits eine Rolle der Tip-Domäne bei der TNFR2 vermittelten Signaltransduktion und Wirkung in diesem Modell postuliert. Andererseits scheint eine direkte Interaktion von TNF und Parasit für die Immunabwehr unwesentlich. Unter Einbeziehung der *in vitro* erhaltenen Befunde einer durch die Tip-Mutationen beeinträchtigten TNFR2 Stimulation wurde somit hier der Hinweis auf eine essentielle Rolle dieses Rezeptors und die damit verbundene Wirkung der lektinartigen Domäne des TNF erhalten.

In der gegenseitigen Wechselwirkung zwischen Wirt und Parasiten im Verlauf von *Trypanosoma brucei* Infektionen *in vivo* jedoch, ist die Lektin-Domäne involviert. In TNFR2 k.o. Mäusen, in denen TNF nicht durch löslichen TNFR2 neutralisiert werden kann, waren diese Befunde sogar noch verstärkt. Daraus wurde gefolgert, dass die trypanolytische Aktivität von TNF *in vitro* in diesem Zusammenhang keine nennenswerte Rolle spielt. Eine Beteiligung von TNF an der von Trypanosomen verursachten Immunsuppression erscheint dagegen als Grund für die erhöhte Parasitämie in TNFR2 k.o. Mäusen näher liegend. Da die TNFR2 vermittelte Bioaktivität der TNF Mutante im Vergleich zu wt TNF vermindert ist, könnte die ausgeprägte Pathologie in den k.i. Mäusen auf eine verminderte Interaktion zwischen TNF und dem neutralisierenden löslichen TNFR2 zurückzuführen sein.

8. References

1 Rouzer CA, Cerami A. Hypertriglyceridemia associated with Trypanosoma brucei brucei infection in rabbits: role of defective triglyceride removal. *Mol Biochem Parasitol* 1980; 2: 31-38.

2 Beutler B *et al.* Identity of tumour necrosis factor and the macrophage-secreted factor cachectin. *Nature* 1985; 316: 552-554.

3 Torti FM *et al.* A macrophage factor inhibits adipocyte gene expression: an in vitro model of cachexia. *Science* 1985; 229: 867-869.

4 Carswell EA *et al.* An endotoxin-induced serum factor that causes necrosis of tumors. *Proc Natl Acad Sci U S A* 1975; 72: 3666-3670.

5 Echtenacher B, Falk W, Mannel DN, Krammer PH. Requirement of endogenous tumor necrosis factor/cachectin for recovery from experimental peritonitis. *J Immunol* 1990; 145: 3762-3766.

6 Heller RA, Kronke M. Tumor necrosis factor receptor-mediated signaling pathways. *J Cell Biol* 1994; 126: 5-9.

7 Kerr JF, Wyllie AH, Currie AR. Apoptosis: a basic biological phenomenon with wide-ranging implications in tissue kinetics. *Br J Cancer* 1972; 26: 239-257.

8 Famularo G, De Simone C, Tzantzoglou S, Trinchieri V. Apoptosis, anti-apoptotic compounds and TNF-alpha release. *Immunol Today* 1994; 15: 495-496.

9 Ware CF, VanArsdale S, VanArsdale TL. Apoptosis mediated by the TNF-related cytokine and receptor families. *J Cell Biochem* 1996; 60: 47-55.

10 Cheng B, Christakos S, Mattson MP. Tumor necrosis factors protect neurons against metabolic-excitotoxic insults and promote maintenance of calcium homeostasis. *Neuron* 1994; 12: 139-153.

11 Tancredi V *et al.* Tumor necrosis factor alters synaptic transmission in rat hippocampal slices. *Neurosci Lett* 1992; 146: 176-178.

12 Kramer B, Machleidt T, Wiegmann K, Kronke M. Superantigen-induced transcriptional activation of the human TNF gene promoter in T cells. *J Inflamm* 1995; 45: 183-192.

13 Grau GE *et al.* Tumor necrosis factor (cachectin) as an essential mediator in murine cerebral malaria. *Science* 1987; 237: 1210-1212.

14 Elliott MJ *et al.* Randomised double-blind comparison of chimeric monoclonal antibody to tumour necrosis factor alpha (cA2) versus placebo in rheumatoid arthritis. *Lancet* 1994; 344: 1105-1110.

15 Feldmann M *et al.* TNF alpha is an effective therapeutic target for rheumatoid arthritis. *Ann N Y Acad Sci* 1995; 766: 272-278.

16 Taupin V *et al.* Increased severity of experimental autoimmune encephalomyelitis, chronic macrophage/microglial reactivity, and demyelination in transgenic mice producing tumor necrosis factor-alpha in the central nervous system. *Eur J Immunol* 1997; 27: 905-913.

17 Landow L, Andersen LW. Splanchnic ischaemia and its role in multiple organ failure. *Acta Anaesthesiol Scand* 1994; 38: 626-639.

18 Selmaj K, Raine CS, Cannella B, Brosnan CF. Identification of lymphotoxin and tumor necrosis factor in multiple sclerosis lesions. *J Clin Invest* 1991; 87: 949-954.

19 Raine CS. Multiple sclerosis: TNF revisited, with promise. *Nat Med* 1995; 1: 211-214.

20 Meldrum DR. Tumor necrosis factor in the heart. *Am J Physiol* 1998; 274: R577-595.

21 Rus HG, Niculescu F, Vlaicu R. Tumor necrosis factor-alpha in human arterial wall with atherosclerosis. *Atherosclerosis* 1991; 89: 247-254.

22 Meldrum DR, Donnahoo KK. Role of TNF in mediating renal insufficiency following cardiac surgery: evidence of a postbypass cardiorenal syndrome. *J Surg Res* 1999; 85: 185-199.

23 Hotamisligil GS *et al.* Increased adipose tissue expression of tumor necrosis factor-alpha in human obesity and insulin resistance. *J Clin Invest* 1995; 95: 2409-2415.

24 Peraldi P, Spiegelman B. TNF-alpha and insulin resistance: summary and future prospects. *Mol Cell Biochem* 1998; 182: 169-175.

25 Brynskov J, Nielsen OH, Ahnfelt-Ronne I, Bendtzen K. Cytokines (immunoinflammatory hormones) and their natural regulation in inflammatory bowel disease (Crohn's disease and ulcerative colitis): a review. *Dig Dis* 1994; 12: 290-304.

26 Vilcek J, Feldmann M. Historical review: Cytokines as therapeutics and targets of therapeutics. *Trends Pharmacol Sci* 2004; 25: 201-209.

27 Ghezzi P, Cerami A. Tumor necrosis factor as a pharmacological target. *Methods Mol Med* 2004; 98: 1-8.

28 Kriegler M *et al.* A novel form of TNF/cachectin is a cell surface cytotoxic transmembrane protein: ramifications for the complex physiology of TNF. *Cell* 1988; 53: 45-53.

29 Black RA *et al.* A metalloproteinase disintegrin that releases tumour-necrosis factor-alpha from cells. *Nature* 1997; 385: 729-733.

30 Engelmann H *et al.* Antibodies to a soluble form of a tumor necrosis factor (TNF) receptor have TNF-like activity. *J Biol Chem* 1990; 265: 14497-14504.

31 Grell M *et al.* The transmembrane form of tumor necrosis factor is the prime activating ligand of the 80 kDa tumor necrosis factor receptor. *Cell* 1995; 83: 793-802.

32 Kull FC, Jr., Jacobs S, Cuatrecasas P. Cellular receptor for 125I-labeled tumor necrosis factor: specific binding, affinity labeling, and relationship to sensitivity. *Proc Natl Acad Sci U S A* 1985; 82: 5756-5760.

33 Ryffel B, Mihatsch MJ. TNF receptor distribution in human tissues. *Int Rev Exp Pathol* 1993; 34 Pt B: 149-156.

34 Grell M, and Scheurich, P. Growth Factors and Cytokines in Health and Disease (LeRoith, D., and Bondy, G. P., eds). *JAI Press Inc., Greenwich, CT* 1997: 669-726.

35 Jones SJ *et al.* TNF recruits TRADD to the plasma membrane but not the trans-Golgi network, the principal subcellular location of TNF-R1. *J Immunol* 1999; 162: 1042-1048.

36 Li X, Yang Y, Ashwell JD. TNF-RII and c-IAP1 mediate ubiquitination and degradation of TRAF2. *Nature* 2002; 416: 345-347.

37 Tartaglia LA *et al.* Stimulation of human T-cell proliferation by specific activation of the 75-kDa tumor necrosis factor receptor. *J Immunol* 1993; 151: 4637-4641.

38 Zheng L *et al.* Induction of apoptosis in mature T cells by tumour necrosis factor. *Nature* 1995; 377: 348-351.

39 Vandenabeele P *et al.* Functional characterization of the human tumor necrosis factor receptor p75 in a transfected rat/mouse T cell hybridoma. *J Exp Med* 1992; 176: 1015-1024.

40 Tartaglia LA, Pennica D, Goeddel DV. Ligand passing: the 75-kDa tumor necrosis factor (TNF) receptor recruits TNF for signaling by the 55-kDa TNF receptor. *J Biol Chem* 1993; 268: 18542-18548.

41 Hsu H, Shu HB, Pan MG, Goeddel DV. TRADD-TRAF2 and TRADD-FADD interactions define two distinct TNF receptor 1 signal transduction pathways. *Cell* 1996; 84: 299-308.

42 Wajant H, Scheurich P. Tumor necrosis factor receptor-associated factor (TRAF) 2 and its role in TNF signaling. *Int J Biochem Cell Biol* 2001; 33: 19-32.

43 Bemelmans MH, Gouma DJ, Buurman WA. LPS-induced sTNF-receptor release in vivo in a murine model. Investigation of the role of tumor necrosis factor,

IL-1, leukemia inhibiting factor, and IFN-gamma. *J Immunol* 1993; 151: 5554-5562.

44 Himmler A *et al.* Molecular cloning and expression of human and rat tumor necrosis factor receptor chain (p60) and its soluble derivative, tumor necrosis factor-binding protein. *DNA Cell Biol* 1990; 9: 705-715.

45 Nophar Y *et al.* Soluble forms of tumor necrosis factor receptors (TNF-Rs). The cDNA for the type I TNF-R, cloned using amino acid sequence data of its soluble form, encodes both the cell surface and a soluble form of the receptor. *Embo J* 1990; 9: 3269-3278.

46 Fernandez-Botran R, Chilton PM, Ma Y. Soluble cytokine receptors: their roles in immunoregulation, disease, and therapy. *Adv Immunol* 1996; 63: 269-336.

47 Mohler KM *et al.* Soluble tumor necrosis factor (TNF) receptors are effective therapeutic agents in lethal endotoxemia and function simultaneously as both TNF carriers and TNF antagonists. *J Immunol* 1993; 151: 1548-1561.

48 Olsson I *et al.* Tumour necrosis factor (TNF) binding proteins (soluble TNF receptor forms) with possible roles in inflammation and malignancy. *Eur Cytokine Netw* 1993; 4: 169-180.

49 Hession C *et al.* Uromodulin (Tamm-Horsfall glycoprotein): a renal ligand for lymphokines. *Science* 1987; 237: 1479-1484.

50 Sherblom AP, Decker JM, Muchmore AV. The lectin-like interaction between recombinant tumor necrosis factor and uromodulin. *J Biol Chem* 1988; 263: 5418-5424.

51 Lucas R *et al.* Mapping the lectin-like activity of tumor necrosis factor. *Science* 1994; 263: 814-817.

52 Magez S *et al.* A conserved flagellar pocket exposed high mannose moiety is used by African trypanosomes as a host cytokine binding molecule. *J Biol Chem* 2001; 276: 33458-33464.

53 Magez S *et al.* Specific uptake of tumor necrosis factor-alpha is involved in growth control of Trypanosoma brucei. *J Cell Biol* 1997; 137: 715-727.

54 Lucas R *et al.* Generation of a mouse tumor necrosis factor mutant with antiperitonitis and desensitization activities comparable to those of the wild type but with reduced systemic toxicity. *Infect Immun* 1997; 65: 2006-2010.

55 Hribar M *et al.* The lectin-like domain of tumor necrosis factor-alpha increases membrane conductance in microvascular endothelial cells and peritoneal macrophages. *Eur J Immunol* 1999; 29: 3105-3111.

56 Fukuda N *et al.* Mechanisms of TNF-alpha stimulation of amiloride-sensitive sodium transport across alveolar epithelium. *Am J Physiol Lung Cell Mol Physiol* 2001; 280: L1258-1265.

57 Matthay MA, Clerici C, Saumon G. Invited review: Active fluid clearance from the distal air spaces of the lung. *J Appl Physiol* 2002; 93: 1533-1541.

58 Elia N *et al.* Functional identification of the alveolar edema reabsorption activity of murine tumor necrosis factor-alpha. *Am J Respir Crit Care Med* 2003; 168: 1043-1050.

59 Matthay MA, Folkesson HG, Clerici C. Lung epithelial fluid transport and the resolution of pulmonary edema. *Physiol Rev* 2002; 82: 569-600.

60 Al-Bazzaz FJ. Regulation of Na and Cl transport in sheep distal airways. *Am J Physiol* 1994; 267: L193-198.

61 Ballard ST *et al.* Regional bioelectric properties of porcine airway epithelium. *J Appl Physiol* 1992; 73: 2021-2027.

62 Inglis SK, Corboz MR, Taylor AE, Ballard ST. Regulation of ion transport across porcine distal bronchi. *Am J Physiol* 1996; 270: L289-297.

63 Staub NC, Albertine KH. The structure of the lungs relative to their principal function. In: Murray JF, Nadel JA (eds). *Textbook of Respiratory Medicine*. Saunders: Philadelphia, 1988, pp. 12-36.

64 Weibel ER. Lung morphometrie and models in respiratory physiology. In: Chang HK, Paiva M (eds). *Respiratory Physiology. An Analytical Approach*. Dekker: New York, 1989, pp. 1-56.

65 Schneeberger EE, Walters DV, Olver RE. Development of intercellular junctions in the pulmonary epithelium of the foetal lamb. *J Cell Sci* 1978; 32: 307-324.

66 Olver RE, Schneeberger EE, Walters DV. Epithelial solute permeability, ion transport and tight junction morphology in the developing lung of the fetal lamb. *J Physiol* 1981; 315: 395-412.

67 Williams M. The alveolar epithelium: structure and study by immunocytochemistry. In: Scharaufagel DE, editor. Electron microscopy of the lung, lung biology in health and disease. New York: Marcel Dekker. 1990: 121-146.

68 Carson JL *et al.* Connexin 26 expression in human and ferret airways and lung during development. *Am J Respir Cell Mol Biol* 1998; 18: 111-119.

69 Abraham V, Chou ML, DeBolt KM, Koval M. Phenotypic control of gap junctional communication by cultured alveolar epithelial cells. *Am J Physiol* 1999; 276: L825-834.

70 Lee YC *et al.* Expression of functional gap junctions in cultured pulmonary alveolar epithelial cells. *Am J Physiol* 1997; 272: L1105-1114.

71 Evans MJ SR, Freeman G. Renewal of pulmonary epithelium following oxidant injury. In: Bouhuyss A, editor. Lung cells in disease. *Amsterdam, The Netherlands: North-Holland* 1976: 165-178.

72 Clerici C. Sodium transport in alveolar epithelial cells: modulation by O2 tension. *Kidney Int Suppl* 1998; 65: S79-83.

73 Goodman B. Ms B and legal competence: examining the role of nurses in difficult ethico-legal decision-making. *Nurs Crit Care* 2003; 8: 78-83.

74 Mason RJ *et al.* Transepithelial transport by pulmonary alveolar type II cells in primary culture. *Proc Natl Acad Sci U S A* 1982; 79: 6033-6037.

75 Matalon S, Benos DJ, Jackson RM. Biophysical and molecular properties of amiloride-inhibitable Na+ channels in alveolar epithelial cells. *Am J Physiol* 1996; 271: L1-22.

76 Matthay MA, Folkesson HG, Verkman AS. Salt and water transport across alveolar and distal airway epithelia in the adult lung. *Am J Physiol* 1996; 270: L487-503.

77 Michaut P *et al.* Rat lung alveolar type II cell line maintains sodium transport characteristics of primary culture. *J Cell Physiol* 1996; 169: 78-86.

78 Skou JC, Esmann M. The Na,K-ATPase. *J Bioenerg Biomembr* 1992; 24: 249-261.

79 Sznajder JI, Olivera WG, Ridge KM, Rutschman DH. Mechanisms of lung liquid clearance during hyperoxia in isolated rat lungs. *Am J Respir Crit Care Med* 1995; 151: 1519-1525.

80 Blanco G *et al.* The alpha-subunit of the Na,K-ATPase has catalytic activity independent of the beta-subunit. *J Biol Chem* 1994; 269: 23420-23425.

81 McDonough AA, Geering K, Farley RA. The sodium pump needs its beta subunit. *Faseb J* 1990; 4: 1598-1605.

82 Goodman BE, Kim KJ, Crandall ED. Evidence for active sodium transport across alveolar epithelium of isolated rat lung. *J Appl Physiol* 1987; 62: 2460-2466.

83 Berthiaume Y *et al.* Alveolar liquid and protein clearance from normal dog lungs. *J Appl Physiol* 1988; 65: 585-593.

84 Berthiaume Y, Staub NC, Matthay MA. Beta-adrenergic agonists increase lung liquid clearance in anesthetized sheep. *J Clin Invest* 1987; 79: 335-343.

85 Fukuda N, Folkesson HG, Matthay MA. Relationship of interstitial fluid volume to alveolar fluid clearance in mice: ventilated vs. in situ studies. *J Appl Physiol* 2000; 89: 672-679.

86 Garat C, Carter EP, Matthay MA. New in situ mouse model to quantify alveolar epithelial fluid clearance. *J Appl Physiol* 1998; 84: 1763-1767.

87 Norlin A, Finley N, Abedinpour P, Folkesson HG. Alveolar liquid clearance in the anesthetized ventilated guinea pig. *Am J Physiol* 1998; 274: L235-243.

88 Sakuma T *et al.* Alveolar fluid clearance in the resected human lung. *Am J Respir Crit Care Med* 1994; 150: 305-310.

89 Sakuma T *et al.* Beta-adrenergic agonist stimulated alveolar fluid clearance in ex vivo human and rat lungs. *Am J Respir Crit Care Med* 1997; 155: 506-512.

90 Crandall ED, Heming TA, Palombo RL, Goodman BE. Effects of terbutaline on sodium transport in isolated perfused rat lung. *J Appl Physiol* 1986; 60: 289-294.

91 Saumon G, Basset G, Bouchonnet F, Crone C. cAMP and beta-adrenergic stimulation of rat alveolar epithelium. Effects on fluid absorption and paracellular permeability. *Pflugers Arch* 1987; 410: 464-470.

92 Icard P, Saumon G. Alveolar sodium and liquid transport in mice. *Am J Physiol* 1999; 277: L1232-1238.

93 Tibayan FA *et al.* Dobutamine increases alveolar liquid clearance in ventilated rats by beta-2 receptor stimulation. *Am J Respir Crit Care Med* 1997; 156: 438-444.

94 Saldias F *et al.* Modulation of lung liquid clearance by isoproterenol in rat lungs. *Am J Physiol* 1998; 274: L694-701.

95 Modelska K, Matthay MA, McElroy MC, Pittet JF. Upregulation of alveolar liquid clearance after fluid resuscitation for hemorrhagic shock in rats. *Am J Physiol* 1997; 273: L305-314.

96 Pittet JF *et al.* Stimulation of lung epithelial liquid clearance by endogenous release of catecholamines in septic shock in anesthetized rats. *J Clin Invest* 1994; 94: 663-671.

97 Jayr C *et al.* Alveolar liquid and protein clearance in anesthetized ventilated rats. *J Appl Physiol* 1994; 76: 2636-2642.

98 Goodman BE, Anderson JL, Clemens JW. Evidence for regulation of sodium transport from airspace to vascular space by cAMP. *Am J Physiol* 1989; 257: L86-93.

99 Saumon G, Basset G. Electrolyte and fluid transport across the mature alveolar epithelium. *J Appl Physiol* 1993; 74: 1-15.

100 Lazrak A, Nielsen VG, Matalon S. Mechanisms of increased Na(+) transport in ATII cells by cAMP: we agree to disagree and do more experiments. *Am J Physiol Lung Cell Mol Physiol* 2000; 278: L233-238.

101 Suzuki S, Zuege D, Berthiaume Y. Sodium-independent modulation of Na(+)-K(+)-ATPase activity by beta-adrenergic agonist in alveolar type II cells. *Am J Physiol* 1995; 268: L983-990.

102 Lasnier JM *et al.* Terbutaline stimulates alveolar fluid resorption in hyperoxic lung injury. *J Appl Physiol* 1996; 81: 1723-1729.

103 Marunaka Y, Niisato N, O'Brodovich H, Eaton DC. Regulation of an amiloride-sensitive Na+-permeable channel by a beta2-adrenergic agonist, cytosolic Ca2+ and Cl- in fetal rat alveolar epithelium. *J Physiol* 1999; 515 (Pt 3): 669-683.

104 Chen XJ, Eaton DC, Jain L. Beta-adrenergic regulation of amiloride-sensitive lung sodium channels. *Am J Physiol Lung Cell Mol Physiol* 2002; 282: L609-620.

105 Jiang X, Ingbar DH, O'Grady SM. Adrenergic stimulation of Na+ transport across alveolar epithelial cells involves activation of apical Cl- channels. *Am J Physiol* 1998; 275: C1610-1620.

106 Jiang X, Ingbar DH, O'Grady SM. Adrenergic regulation of ion transport across adult alveolar epithelial cells: effects on Cl- channel activation and transport

function in cultures with an apical air interface. *J Membr Biol* 2001; 181: 195-204.

107 Snyder PM. Liddle's syndrome mutations disrupt cAMP-mediated translocation of the epithelial Na(+) channel to the cell surface. *J Clin Invest* 2000; 105: 45-53.

108 Matthay MA, Folkesson HG, Clerici C. Lung epithelial fluid transport and the resolution of pulmonary edema. *Physiol Rev* 2002; 82: 569-600.

109 Crandall ED, Matthay MA. Alveolar epithelial transport. Basic science to clinical medicine. *Am J Respir Crit Care Med* 2001; 163: 1021-1029.

110 Dematte JE, Sznajder JI. Mechanisms of pulmonary edema clearance: from basic research to clinical implication. *Intensive Care Med* 2000; 26: 477-480.

111 Matthay MA *et al.* Alveolar epithelial barrier. Role in lung fluid balance in clinical lung injury. *Clin Chest Med* 2000; 21: 477-490.

112 Beutler B. Endotoxin, tumor necrosis factor, and related mediators: new approaches to shock. *New Horiz* 1993; 1: 3-12.

113 Royall D *et al.* Continuous measurement of energy expenditure in ventilated burn patients: an analysis. *Crit Care Med* 1994; 22: 399-406.

114 Shimomoto H *et al.* Expression of tumor necrosis factor receptors in human lung cancer cells and normal lung tissues. *Am J Respir Cell Mol Biol* 1995; 13: 271-278.

115 Smith S *et al.* The locus of tumor necrosis factor-alpha action in lung inflammation. *Am J Respir Cell Mol Biol* 1998; 19: 881-891.

116 Vassalli P. The pathophysiology of tumor necrosis factors. *Annu Rev Immunol* 1992; 10: 411-452.

117 Ware CF, VanArsdale TL, Crowe PD, Browning JL. The ligands and receptors of the lymphotoxin system. *Curr Top Microbiol Immunol* 1995; 198: 175-218.

118 O'Grady NP *et al.* Local inflammatory responses following bronchial endotoxin instillation in humans. *Am J Respir Crit Care Med* 2001; 163: 1591-1598.

119 Clowes GH, Jr. *et al.* Septic lung and shock lung in man. *Ann Surg* 1975; 181: 681-692.

120 Lecuona E *et al.* Ventilator-associated lung injury decreases lung ability to clear edema in rats. *Am J Respir Crit Care Med* 1999; 159: 603-609.

121 Modelska K *et al.* Acid-induced lung injury. Protective effect of anti-interleukin-8 pretreatment on alveolar epithelial barrier function in rabbits. *Am J Respir Crit Care Med* 1999; 160: 1450-1456.

122 Laffon M *et al.* Interleukin-8 mediates injury from smoke inhalation to both the lung endothelial and the alveolar epithelial barriers in rabbits. *Am J Respir Crit Care Med* 1999; 160: 1443-1449.

123 Lo SK, Everitt J, Gu J, Malik AB. Tumor necrosis factor mediates experimental pulmonary edema by ICAM-1 and CD18-dependent mechanisms. *J Clin Invest* 1992; 89: 981-988.

124 Calkins CM *et al.* TNF receptor I mediates chemokine production and neutrophil accumulation in the lung following systemic lipopolysaccharide. *J Surg Res* 2001; 101: 232-237.

125 Horgan MJ, Palace GP, Everitt JE, Malik AB. TNF-alpha release in endotoxemia contributes to neutrophil-dependent pulmonary edema. *Am J Physiol* 1993; 264: H1161-1165.

126 Khimenko PL, Bagby GJ, Fuseler J, Taylor AE. Tumor necrosis factor-alpha in ischemia and reperfusion injury in rat lungs. *J Appl Physiol* 1998; 85: 2005-2011.

127 Rezaiguia S *et al.* Acute bacterial pneumonia in rats increases alveolar epithelial fluid clearance by a tumor necrosis factor-alpha-dependent mechanism. *J Clin Invest* 1997; 99: 325-335.

128 Borjesson A *et al.* TNF-alpha stimulates alveolar liquid clearance during intestinal ischemia-reperfusion in rats. *Am J Physiol Lung Cell Mol Physiol* 2000; 278: L3-12.

129 Braun C. Tumor Necrosis Factor: The Yin and Yang of Pulmonary Oedema. *Hartung-Gorre Verlag* 2003.

130 Vickerman K, Tetley L, Hendry KA, Turner CM. Biology of African trypanosomes in the tsetse fly. *Biol Cell* 1988; 64: 109-119.

131 Organization WH. Control and surveillance of Afrcan trypanosomiases: report of a WHO Expert Commitee. *World Health Organ Tech Rep Ser* 1998; 881: 1-114.

132 Kristjanson PM SB, Rowlands GJ, Kruska RL, de Leeuw PN. Measuring the cost of African trypanosomiasis: the potential benefits of control and returns to research. *Agric. Syst* 1999; 59: 79-98.

133 MacLean L, Odiit M, Sternberg JM. Nitric oxide and cytokine synthesis in human African trypanosomiasis. *J Infect Dis* 2001; 184: 1086-1090.

134 Lucas R *et al.* A role for TNF during African trypanosomiasis: involvement in parasite control, immunosuppression and pathology. *Res Immunol* 1993; 144: 370-376.

135 Donelson JE. Antigenic variation and the African trypanosome genome. *Acta Trop* 2003; 85: 391-404.

136 Jackson DG, Owen MJ, Voorheis HP. A new method for the rapid purification of both the membrane-bound and released forms of the variant surface glycoprotein from Trypanosoma brucei. *Biochem J* 1985; 230: 195-202.

137 Cross GA. Cellular and genetic aspects of antigenic variation in trypanosomes. *Annu Rev Immunol* 1990; 8: 83-110.

138 Pays E, Vanhamme L, Berberof M. Genetic controls for the expression of surface antigens in African trypanosomes. *Annu Rev Microbiol* 1994; 48: 25-52.

139 Turner CM. Antigenic variation in Trypanosoma brucei infections: an holistic view. *J Cell Sci* 1999; 112 (Pt 19): 3187-3192.

140 Barry JD. The biology of antigenic variation in African trypanosomes. In *Trypanosomiasis and Leishmaniasis.* (ed. G. Hide, J. C. Mottram; G. H. Coombs and P. H. Holmes). *Cab International. Oxford, United Kingdom* 1997: 89-107.

141 Murray M, Morrison WI, Whitelaw DD. Host susceptibility to African trypanosomiasis: trypanotolerance. *Adv Parasitol* 1982; 21: 1-68.

142 Pinder M. Trypanosoma congolense: genetic control of resistance to infection in mice. *Exp Parasitol* 1984; 57: 185-194.

143 Uzonna JE, Kaushik RS, Gordon JR, Tabel H. Immunoregulation in experimental murine Trypanosoma congolense infection: anti-IL-10 antibodies reverse trypanosome-mediated suppression of lymphocyte proliferation in vitro and moderately prolong the lifespan of genetically susceptible BALB/c mice. *Parasite Immunol* 1998; 20: 293-302.

144 Ogunremi O, Tabel H. Genetics of resistance to Trypanosoma congolense in inbred mice: efficiency of apparent clearance of parasites correlates with long-term survival. *J Parasitol* 1995; 81: 876-881.

145 Black SJ *et al.* Regulation of the growth and differentiation of Trypanosoma (Trypanozoon) brucei brucei in resistant (C57Bl/6) and susceptible (C3H/He) mice. *Parasite Immunol* 1983; 5: 465-478.

146 Levine RF, Mansfield JM. Genetics of resistance to African trypanosomes: role of the H-2 locus in determining resistance to infection with Trypanosoma rhodesiense. *Infect Immun* 1981; 34: 513-518.

147 Greenblatt HC, Diggs CL, Rosenstreich DL. Trypanosoma rhodesiense: analysis of the genetic control of resistance among mice. *Infect Immun* 1984; 44: 107-111.

148 Okomo-Assoumou MC *et al.* Correlation of high serum levels of tumor necrosis factor-alpha with disease severity in human African trypanosomiasis. *Am J Trop Med Hyg* 1995; 53: 539-543.

149 Paulnock DM, Demick KP, Coller SP. Analysis of interferon-gamma-dependent and -independent pathways of macrophage activation. *J Leukoc Biol* 2000; 67: 677-682.

150 de Gee AL, Sonnenfeld G, Mansfield JM. Genetics of resistance to the African trypanosomes. V. Qualitative and quantitative differences in interferon production among susceptible and resistant mouse strains. *J Immunol* 1985; 134: 2723-2726.

151 Hertz CJ, Filutowicz H, Mansfield JM. Resistance to the African trypanosomes is IFN-gamma dependent. *J Immunol* 1998; 161: 6775-6783.

152 Magez S *et al.* Murine tumour necrosis factor plays a protective role during the initial phase of the experimental infection with Trypanosoma brucei brucei. *Parasite Immunol* 1993; 15: 635-641.

153 Magez S *et al.* Tumor necrosis factor alpha is a key mediator in the regulation of experimental Trypanosoma brucei infections. *Infect Immun* 1999; 67: 3128-3132.

154 de Gee AL, McCann PP, Mansfield JM. Role of antibody in the elimination of trypanosomes after DL-alpha-difluoromethylornithine chemotherapy. *J Parasitol* 1983; 69: 818-822.

155 De Gee AL, Levine RF, Mansfield JM. Genetics of resistance to the African trypanosomes. VI. Heredity of resistance and variable surface glycoprotein-specific immune responses. *J Immunol* 1988; 140: 283-288.

156 Sileghem M, Flynn JN, Logan-Henfrey L, Ellis J. Tumour necrosis factor production by monocytes from cattle infected with Trypanosoma (Duttonella) vivax and Trypanosoma (Nannomonas) congolense: possible association with severity of anaemia associated with the disease. *Parasite Immunol* 1994; 16: 51-54.

157 Lejon V *et al.* Interleukin (IL)-6, IL-8 and IL-10 in serum and CSF of Trypanosoma brucei gambiense sleeping sickness patients before and after treatment. *Trans R Soc Trop Med Hyg* 2002; 96: 329-333.

158 Magez S *et al.* P75 tumor necrosis factor-receptor shedding occurs as a protective host response during African trypanosomiasis. *J Infect Dis* 2004; 189: 527-539.

159 Edelhoch H. Spectroscopic determination of tryptophan and tyrosine in proteins. *Biochemistry* 1967; 6: 1948-1954.

160 Serikov VB, Grady M, Matthay MA. Effect of temperature on alveolar liquid and protein clearance in an in situ perfused goat lung. *J Appl Physiol* 1993; 75: 940-947.

161 Krippner-Heidenreich A *et al.* Control of receptor-induced signaling complex formation by the kinetics of ligand/receptor interaction. *J Biol Chem* 2002; 277: 44155-44163.

162 Grell M, Scheurich P, Meager A, Pfizenmaier K. TR60 and TR80 tumor necrosis factor (TNF)-receptors can independently mediate cytolysis. *Lymphokine Cytokine Res* 1993; 12: 143-148.

163 Zhang XM, Weber I, Chen MJ. Site-directed mutational analysis of human tumor necrosis factor-alpha receptor binding site and structure-functional relationship. *J Biol Chem* 1992; 267: 24069-24075.

164 Dudich E *et al.* alpha-fetoprotein causes apoptosis in tumor cells via a pathway independent of CD95, TNFR1 and TNFR2 through activation of caspase-3-like proteases. *Eur J Biochem* 1999; 266: 750-761.

165 Hribar M *et al.* The lectin-like domain of tumor necrosis factor-alpha increases membrane conductance in microvascular endothelial cells and peritoneal macrophages. *Eur J Immunol* 1999; 29: 3105-3111.

166 Fukuda N *et al.* Mechanisms of TNF-alpha stimulation of amiloride-sensitive sodium transport across alveolar epithelium. *Am J Physiol Lung Cell Mol Physiol* 2001; 280: L1258-1265.

167 Sakuma T *et al.* The granulocyte colony-stimulating factor produced in the human lung and its effect on liquid movement in the rabbit lung. *Surg Today* 1994; 24: 1050-1055.

168 Dreyfuss D, Saumon G. Ventilator-induced lung injury: lessons from experimental studies. *Am J Respir Crit Care Med* 1998; 157: 294-323.

169 Parker JC, Hernandez LA, Peevy KJ. Mechanisms of ventilator-induced lung injury. *Crit Care Med* 1993; 21: 131-143.

170 Slutsky AS, Tremblay LN. Multiple system organ failure. Is mechanical ventilation a contributing factor? *Am J Respir Crit Care Med* 1998; 157: 1721-1725.

171 Chiumello D, Pristine G, Slutsky AS. Mechanical ventilation affects local and systemic cytokines in an animal model of acute respiratory distress syndrome. *Am J Respir Crit Care Med* 1999; 160: 109-116.

172 Imai Y *et al.* Intratracheal anti-tumor necrosis factor-alpha antibody attenuates ventilator-induced lung injury in rabbits. *J Appl Physiol* 1999; 87: 510-515.

173 Imai Y *et al.* Inflammatory chemical mediators during conventional ventilation and during high frequency oscillatory ventilation. *Am J Respir Crit Care Med* 1994; 150: 1550-1554.

174 Ranieri VM *et al.* Effect of mechanical ventilation on inflammatory mediators in patients with acute respiratory distress syndrome: a randomized controlled trial. *Jama* 1999; 282: 54-61.

175 Stuber F *et al.* Kinetic and reversibility of mechanical ventilation-associated pulmonary and systemic inflammatory response in patients with acute lung injury. *Intensive Care Med* 2002; 28: 834-841.

176 Sugiura M *et al.* Ventilator pattern influences neutrophil influx and activation in atelectasis-prone rabbit lung. *J Appl Physiol* 1994; 77: 1355-1365.

177 Imai Y *et al.* Comparison of lung protection strategies using conventional and high-frequency oscillatory ventilation. *J Appl Physiol* 2001; 91: 1836-1844.

178 Takata K, Horiuchi S, Morino Y. Scavenger receptor-mediated recognition of maleylated albumin and its relation to subsequent endocytic degradation. *Biochim Biophys Acta* 1989; 984: 273-280.

179 Wilson MR *et al.* High tidal volume upregulates intrapulmonary cytokines in an in vivo mouse model of ventilator-induced lung injury. *J Appl Physiol* 2003; 95: 1385-1393.

180 Beutler B, Cerami A. Tumor necrosis, cachexia, shock, and inflammation: a common mediator. *Annu Rev Biochem* 1988; 57: 505-518.

181 Dempsey WL, Mansfield JM. Lymphocyte function in experimental African trypanosomiasis. V. Role of antibody and the mononuclear phagocyte system in variant-specific immunity. *J Immunol* 1983; 130: 405-411.

182 Pasparakis M, Alexopoulou L, Episkopou V, Kollias G. Immune and inflammatory responses in TNF alpha-deficient mice: a critical requirement for TNF alpha in the formation of primary B cell follicles, follicular dendritic cell networks and germinal centers, and in the maturation of the humoral immune response. *J Exp Med* 1996; 184: 1397-1411.

183 Rezaiguia S *et al.* Acute bacterial pneumonia in rats increases alveolar epithelial fluid clearance by a tumor necrosis factor-alpha-dependent mechanism. *J Clin Invest* 1997; 99: 325-335.

184 Borjesson A *et al.* TNF-alpha stimulates alveolar liquid clearance during intestinal ischemia-reperfusion in rats. *Am J Physiol Lung Cell Mol Physiol* 2000; 278: L3-12.

185 Berthiaume Y. Effect of exogenous cAMP and aminophylline on alveolar and lung liquid clearance in anesthetized sheep. *J Appl Physiol* 1991; 70: 2490-2497.

186 Charron PD, Fawley JP, Maron MB. Effect of epinephrine on alveolar liquid clearance in the rat. *J Appl Physiol* 1999; 87: 611-618.

187 Pittet JF *et al.* Stimulation of lung epithelial liquid clearance by endogenous release of catecholamines in septic shock in anesthetized rats. *J Clin Invest* 1994; 94: 663-671.

188 Lucas S. Initial Abortive Treatments for Migraine Headache. *Curr Treat Options Neurol* 2002; 4: 343-350.

189 Folkesson HG, Pittet JF, Nitenberg G, Matthay MA. Transforming growth factor-alpha increases alveolar liquid clearance in anesthetized ventilated rats. *Am J Physiol* 1996; 271: L236-244.

190 Hunter CA *et al.* Immunopathology of experimental African sleeping sickness: detection of cytokine mRNA in the brains of Trypanosoma brucei brucei-infected mice. *Infect Immun* 1991; 59: 4636-4640.

191 Darji A *et al.* Mechanisms underlying trypanosome-elicited immunosuppression. *Ann Soc Belg Med Trop* 1992; 72 Suppl 1: 27-38.

192 Truyens C *et al.* The cachexia associated with Trypanosoma cruzi acute infection in mice is attenuated by anti-TNF-alpha, but not by anti-IL-6 or anti-IFN-gamma antibodies. *Parasite Immunol* 1995; 17: 561-568.

193 Schmidt H, Bafort JM. African trypanosomiasis: haematogenic brain parasitism early in experimental infection through bypassing the blood-brain barrier, with considerations on brain trypanosomiasis in man. *Parasitol Res* 1987; 73: 15-21.

194 Mulenga C, Mhlanga JD, Kristensson K, Robertson B. Trypanosoma brucei brucei crosses the blood-brain barrier while tight junction proteins are

preserved in a rat chronic disease model. *Neuropathol Appl Neurobiol* 2001; 27: 77-85.

195 Darji A *et al.* In vitro simulation of immunosuppression caused by Trypanosoma brucei: active involvement of gamma interferon and tumor necrosis factor in the pathway of suppression. *Infect Immun* 1996; 64: 1937-1943.